Journal of Computational Physics 228 (2009) 1030–1055

Contents lists available at ScienceDirect

Journal of Computational Physics

journal homepage: www.elsevier.com/locate/jcp

Calculating effective diffusivities in the limit of vanishing molecular diffusion

G.A. Pavliotis [a], A.M. Stuart [b], K.C. Zygalakis [b,*]

[a] Department of Mathematics, Imperial College, London SW7 2AZ, United Kingdom
[b] Mathematics Institute, University of Warwick, Coventry CV4 7AL, United Kingdom

ARTICLE INFO

Article history:
Received 19 June 2008
Received in revised form 9 October 2008
Accepted 10 October 2008
Available online 22 October 2008

MSC:
60H10
60H30
74H40
34E13

Keywords:
Homogenization theory
Multiscale analysis
Monte Carlo methods
Passive tracers
Inertial particles
Effective diffusivity

ABSTRACT

In this paper we study the problem of the numerical calculation (by Monte Carlo methods) of the effective diffusivity for a particle moving in a periodic divergent-free velocity field, in the limit of vanishing molecular diffusion. In this limit traditional numerical methods typically fail, since they do not represent accurately the geometry of the underlying deterministic dynamics. We propose a stochastic splitting method that takes into account the volume-preserving property of the equations of motion in the absence of noise, and when inertial effects can be neglected. An extension of the method is then proposed for the cases where the noise has a non-trivial time-correlation structure and when inertial effects cannot be neglected. The method of modified equations is used to explain failings of Euler-based methods. The new stochastic geometric integrators are shown to outperform standard Euler-based integrators. Various asymptotic limits of physical interest are investigated by means of numerical experiments, using the new integrators.

1. Introduction

Understanding the transport properties of particles moving in fluid flows and subject to molecular diffusion is a problem of great theoretical and practical importance [7,13] with applications in, for example, atmosphere/ocean science and chemical engineering [5,31,19]. In the case where inertial effects can be neglected, the equation of motion for the particle is

$$\dot{x} = v(x,t) + \sigma\dot{W}. \tag{1.1}$$

Here, $x \in \mathbb{R}^d$, W is a standard d-dimensional Brownian motion, $v(x,t)$ is the fluid velocity field (which we take to be incompressible) and σ the molecular diffusivity. We will refer to this equation as the *passive tracers model*.

It can be shown using multiscale/homogenization techniques [2,22], that when the velocity field $v(x,t)$ is either periodic or random with sufficiently good mixing properties, the long time, large scale dynamics of (1.1) is governed by an effective Brownian motion with a non-negative covariance matrix, the *effective diffusion tensor* or *effective diffusivity*. The calculation of

* Corresponding author.
E-mail addresses: g.pavliotis@imperial.ac.uk (G.A. Pavliotis), A.M.Stuart@warwick.ac.uk (A.M. Stuart), K.C.Zygalakis@warwick.ac.uk (K.C. Zygalakis).

0021-9991/$ - see front matter © 2008 Elsevier Inc. All rights reserved.
doi:10.1016/j.jcp.2008.10.014

the effective diffusivity, in the case where the velocity field is a smooth periodic field, requires the solution of an appropriate boundary value problem, the *cell problem*, together with the calculation of an integral over the period of the velocity field [22, Chapter 13]. Similar results hold for random, time dependent velocity fields [3].

Various properties of the effective diffusivity have been investigated. In particular, it has been shown that the effective diffusivity is always enhanced over bare molecular diffusivity for incompressible flows [18,13,9], while it is always depleted for potential flows, [36] (see [22, Chapter 13] for a discussion). Furthermore, the scaling of the effective diffusivity with respect to the bare molecular diffusion σ, in particular in the physically interesting regime $\sigma \ll 1$, has been studied extensively in the literature. It has been shown that the scaling of the diffusion coefficient with σ depends crucially on the streamline topology [9,13,35,32]. For example, for steady flows with closed streamlines the effective diffusivity scales like σ, as $\sigma \to 0$, whereas for flows with open streamlines (shear flows) it scales like $1/\sigma^2$ [12]. Note that for $v = 0$ the diffusivity scales like σ^2.

There are various physical applications where modeling the noise in Eq. (1.1) as delta correlated in time is inadequate. As an example we mention the problem of transport of passive scalars in the ocean; in this case the noise comes from the unresolved velocity scales which are correlated in time [4]. A simple variant of Eq. (1.1) where the noise process has a non-trivial correlation structure is

$$\dot{x} = v(x,t) + \sigma\eta, \tag{1.2}$$

where η is a d-dimensional Ornstein–Uhlenbeck process with exponential correlation function,

$$\langle \eta_i(t)\eta_j(s)\rangle = \delta_{ij} e^{-\frac{|t-s|}{\delta}}, \quad i,j = 1,\dots d.$$

We will refer to this problem as the *coloured noise* problem for passive tracers. It is still possible to show, using multiscale/homogenization techniques, that the long time, large scale behaviour solutions to Eq. (1.2) is governed by an effective Brownian motion with effective diffusivity D [38].

On the other hand, there exist various applications where inertial effects cannot be ignored. As examples we mention rain formation [6,31] and suspensions of biological organisms in the ocean. Recently there has been a burst of activity on the theoretical and numerical study of various mathematical models for the motion of inertial particles in laminar and turbulent flows [1,33,34]. The starting point for many theoretical investigations concerning inertial particles is Stokes' law, which says that the force $F_s(t)$ exerted by the fluid on the particle is proportional to the difference between the background fluid velocity and the particle velocity:

$$F_s(t) \propto v(x(t),t) - \dot{x}(t). \tag{1.3}$$

Various extensions of this basic model have been considered in the literature, in particular by Maxey and collaborators [14–17,29,37].

The equation of motion for a particle subject to the force (1.3) and molecular diffusion is

$$\tau\ddot{x} = v(x,t) - \dot{x} + \sigma\dot{W}, \tag{1.4}$$

where $x \in \mathbb{R}^d$, W is a standard d-dimensional Brownian motion and τ is the Stokes number. We will refer to this as the *inertial particles model*. It is possible to show, with the use of multiscale/homogenization techniques, that for either steady periodic or time dependent random velocity fields, the long time, large scale dynamics of solutions to (1.4) is governed by an effective Brownian motion [21,23,25]. For the calculation of the effective diffusion tensor the solution of a boundary value problem is required, together with the calculation of an integral over the phase space $\mathbb{T}^d \times \mathbb{R}^d$.

The effective diffusion coefficient for inertial particles depends in a complicated, highly nonlinear way on the parameters of the problem, such as the Stokes number, the strength of the noise and the velocity correlation time. Very little is known analytically concerning the dependence of the effective diffusivity on these parameters, in contrast to the passive tracers case where this problem has been studied extensively. For example, numerical simulations presented in [23,25] suggest that for incompressible flows the effective diffusivity for inertial particles is always greater than that of passive tracers, but no proof of this result exists. Furthermore, the presence of inertia gives rise to various asymptotic limits of physical interest in addition to the relevant distinguished limits for the passive tracers model, such as taking $\sigma \to 0$ while keeping the Stokes number τ fixed, as well as the limit where $(\sigma,\tau) \to 0$ simultaneously.

Since very little is known analytically for the effective diffusivity, it is instructive to resort to numerical simulations for its calculation. In this paper we use Monte Carlo methods. For the accurate numerical calculation of the diffusion coefficient it is necessary to use numerical methods that can integrate accurately the stochastic equations of motion over long time intervals (i.e. until the system reaches the asymptotic regime described by an effective Brownian motion); furthermore, it is desirable that the numerical method is robust with respect to variations in the parameters of the problem such as the Stokes number and the strength of molecular diffusion. In particular, we want numerical methods which perform well when the parameters in the equations of motion become either very large or very small.

The purpose of this paper is twofold:

(i) We propose new numerical integrators for passive tracers and inertial particles by constructing stochastic generalizations of the geometric integrator proposed in [28]. The idea is to construct integrators by composing a geometric

integrator with the explicit solution of a Gaussian stochastic differential equation. This idea is also used in molecular dynamics: see [20] and the references within.

(ii) Having shown the efficiency of the resulting method for the calculation of the effective diffusivity for passive tracers, we investigate numerically various asymptotic limits of physical interest, including the small Stokes number limit for inertial particles and the coloured noise problem for passive tracers. In addition, we generalize the invariant manifold result for inertial particles in cellular flows [29] to the stochastic case (1.4), by using stochastic averaging.

The rest of this paper is organized as follows. In Section 2 we describe the stochastic geometric integrator for both the passive tracers and inertial particles cases. Section 3 contains some theoretical analysis of the numerical method, more specifically the proof of convergence of the method as well as its behaviour in the limit of small inertia. In Section 4 we summarize various results concerning Eqs. (1.1) and (1.4) in the asymptotic limits $\sigma \to 0$ and $\tau \to 0$. Sections 5–7 contain various numerical investigations of the relevant asymptotic limits highlighted in Section 4. Section 8 is reserved for conclusions. Various technical results are presented in the Appendices.

2. Stochastic geometric integrators

In this section we describe the stochastic splitting method for both passive tracers and inertial particles. Before doing this we describe a special feature of the Taylor–Green velocity field and then describe the numerical method in a general framework abstracting this case.

The Taylor–Green velocity field $v = \nabla^\perp \Psi_{TG}$,[1] $\Psi_{TG} = \sin x_1 \sin x_2$ can be written as

$$v(x_1, x_2) = \begin{pmatrix} -\cos x_2 \sin x_1 \\ \sin x_2 \cos x_1 \end{pmatrix}. \tag{2.1}$$

Using the product formula $\sin\alpha\cos\beta = \frac{1}{2}\sin(\alpha+\beta) + \frac{1}{2}\sin(\alpha-\beta)$, the vector field v can be split as follows:

$$v(x) = d_1 g(\langle e_1, x\rangle) + d_2 g(\langle e_2, x\rangle),$$

where by $\langle\cdot,\cdot\rangle$ we denote the usual inner product on $\mathbb{R}^2$, $g(x) = \sin x$, and

$$e_1 = \begin{pmatrix} 1 \\ 1 \end{pmatrix}, \quad e_2 = \begin{pmatrix} 1 \\ -1 \end{pmatrix}, \quad d_1 = -\frac{1}{2}e_2, \quad d_2 = -\frac{1}{2}e_1. \tag{2.2}$$

The key property of this velocity field is that the vectors d_j, e_j are orthogonal for each j:

$$\langle d_j, e_j\rangle = 0, \quad j = 1, \ldots, n. \tag{2.3}$$

With this in mind we proceed to the analysis of the splitting method in the case where the velocity field can be written as

$$v(x) = \sum_{j=1}^{n} d_j v_j(\langle e_j, x\rangle), \tag{2.4}$$

assuming (2.3) holds. Note that each vector field $d_j v_j(\langle e_j, \cdot\rangle)$ is itself incompressible and integrable because of (2.3). Furthermore, if we consider the ODE

$$\frac{d}{dt}x^j = d_j v_j(\langle e_j, x^j\rangle), \tag{2.5}$$

is easy to check that, by (2.3),

$$\frac{d}{dt}\langle e_j, x^j\rangle = 0. \tag{2.6}$$

Thus flows in the individual vector fields are exactly integrable and

$$x^j(t) = x^j(0) + t d_j v_j(\langle e_j, x^j(0)\rangle). \tag{2.7}$$

Note also that in the Taylor–Green case the vectors are 2-dimensional but the method we describe works for vectors of arbitary finite dimension d. The idea of exploiting the splitting (2.4) to construct volume-preserving integrators for (1.1) with $\sigma = 0$ was introduced in [28].

2.1. Passive tracers

We now describe the stochastic splitting method for velocity fields of the form (2.4) in the passive tracers case. We want to solve the Eq. (1.1). Consider the flow $\phi_j(x,t)$ generated by (2.7):

[1] Here $\nabla^\perp$ stands for $\nabla^\perp = (-\frac{\partial}{\partial x_2}, \frac{\partial}{\partial x_1})$.

$$\phi_j(x,t) = x + td_j v_j\big(\langle e_j, x\rangle\big). \tag{2.8}$$

Note that $\phi_j(x,t)$ is volume-preserving. A numerical approximation of the deterministic part of (1.1) is given by [28]

$$\begin{aligned} &x_{k+1} = \phi(x_k, \Delta t), \\ &\phi(x,t) = (\phi_n \circ \cdots \circ \phi_1)(x,t). \end{aligned} \tag{2.9}$$

As the composition of volume-preserving maps, ϕ is itself a volume-preserving map. To incorporate the stochastic part of Eq. (1.1), we simply set

$$x_{k+1} = \phi(x_k, \Delta t) + \sigma\sqrt{\Delta t}\gamma_k, \tag{2.10}$$

where γ_k are i.i.d vectors with $\gamma_1 \sim \mathcal{N}(0, I_d)$. If we define the random map

$$\psi(x,t,\xi) = \phi(x,t) + \sigma\sqrt{t}\xi, \tag{2.11}$$

then

$$x_{k+1} = \psi(x_k, \Delta t, \gamma_k).$$

2.2. Inertial particles

We now describe the stochastic splitting method for velocity fields with the properties (2.3) and (2.4) in the inertial particle case (1.4). A generalization of the strategy from the previous subsection is as follows. The inertial particles system (1.4) can be written as a first-order system,

$$\dot z = F(z) + \Sigma\dot W,$$

where $z = (x,y)$, and

$$F(z) = \begin{pmatrix} \frac{1}{\sqrt\tau} y \\ \frac{1}{\sqrt\tau}\sum_{j=1}^{n} d_j v_j(\langle e_j, x\rangle) - \frac{1}{\tau} y \end{pmatrix}, \quad \Sigma = \begin{pmatrix} 0 \\ \frac{\sigma}{\sqrt\tau} \end{pmatrix}.$$

The most straightforward splitting would appear to be found by writing $F(z) = \sum_{j=1}^{n+1} F_j(z)$, with

$$F_j(z) = \begin{pmatrix} \frac{1}{n\sqrt\tau} y \\ \frac{1}{\sqrt\tau} d_j v_j(\langle e_j, x\rangle) - \frac{1}{n\tau} y \end{pmatrix}, \quad j = 1, \ldots, n$$

and

$$F_{n+1}(z) = \begin{pmatrix} 0 \\ \frac{\sigma}{\sqrt\tau}\dot W \end{pmatrix},$$

which corresponds to adding a Brownian motion in the last step. However, the resulting splitting methods lead to restrictions on $\Delta t/\tau$, something we wish to avoid. To this end we set

$$F_j(z) = \begin{pmatrix} \frac{1}{(n+1)\sqrt\tau} y \\ \frac{1}{\sqrt\tau} d_j v_j(\langle e_j, x\rangle) - \frac{1}{(n+1)\tau} y \end{pmatrix}, \quad j = 1, \ldots, n$$

and

$$F_{n+1}(z) = \begin{pmatrix} \frac{1}{(n+1)\sqrt\tau} y \\ -\frac{1}{(n+1)\tau} y + \frac{\sigma}{\sqrt\tau}\dot W \end{pmatrix},$$

where the last step now corresponds to an Ornstein–Uhlenbeck process with timescale τ, in y. The deterministic subequations corresponding to this splitting are

$$(n+1)\tau\ddot x^j = d_j v_j(\langle e_j, x^j\rangle) - \dot x^j, \tag{2.12}$$

and the stochastic part is

$$(n+1)\tau\ddot x = -\dot x + \sigma\dot W. \tag{2.13}$$

If we take the inner product with e_j in (2.12) and use (2.4) then we obtain

$$(n+1)\tau\langle e_j, \ddot x^j\rangle + \langle e_j, \dot x^j\rangle = 0, \quad j = 1, \ldots, n.$$

Thus

$$\langle e_j, x^j(t)\rangle = a - b(n+1)\tau \exp\left[-\frac{t}{(n+1)\tau}\right],$$

where

$$a = \langle e_j, x^j(0)\rangle + (n+1)\tau\langle e_j, \dot{x}^j(0)\rangle, \quad b = \langle e_j, \dot{x}^j(0)\rangle.$$

Note that now Eq. (2.12) becomes

$$(n+1)\tau\ddot{x}^j + \dot{x}^j = f_j(t), \quad j = 1, \ldots, n$$

which can be solved explicitly up to quadratures to give the result:

$$\begin{aligned} x^j(t) &= x^j(0) + \frac{1}{(n+1)\sqrt{\tau}}\int_0^t y^j(s)ds, \\ y^j(t) &= y^j(0)\exp\left[-\frac{t}{(n+1)\tau}\right] + \frac{1}{\sqrt{\tau}}\int_0^t \exp\left[-\frac{(t-s)}{(n+1)\tau}\right] f_j(s)ds. \end{aligned} \tag{2.14}$$

Here

$$f_j(t) = d_j v_j(\langle e_j, x^j(t)\rangle) = d_j v_j\left(a - b(n+1)\tau\exp\left[-\frac{t}{(n+1)\tau}\right]\right). \tag{2.15}$$

We denote by $\widehat{\phi}_j(x,y,t)$ the flow generated by (2.14) and (2.15) to obtain a first-order integrator for the noise free dynamics:

$$\widehat{\phi}(x,y,\Delta t) = (\widehat{\phi}_n \circ \cdots \circ \widehat{\phi}_1)(x,y,\Delta t).$$

We now take into consideration the stochastic part of (1.4). From (2.13) we have

$$\dot{x} = \frac{1}{(n+1)\sqrt{\tau}}y, \tag{2.16a}$$

$$\dot{y} = \frac{-1}{(n+1)\tau}y + \frac{\sigma}{\sqrt{\tau}}\dot{W}. \tag{2.16b}$$

It is possible to solve this SDE explicitly to give

$$\begin{pmatrix} x(t) \\ y(t)\end{pmatrix} = \lambda \circ \widehat{\phi}(x(0), y(0), t) + g(\xi, \gamma, t),$$

where $\lambda(x,y,t)$ is defined by

$$\lambda(x,y,t) = \begin{pmatrix} x + \sqrt{\tau}\left(1 - \exp\left[\frac{-t}{(n+1)\tau}\right]\right)y \\ y\exp\left[\frac{-t}{(n+1)\tau}\right]\end{pmatrix},$$

and $g(\gamma, \xi, t)$ describes the noise. It is given by

$$g(\xi, \gamma, t) = \begin{pmatrix} \alpha\xi + \delta\gamma \\ \beta\xi\end{pmatrix}, \tag{2.17}$$

where γ, ξ are i.i.d vectors with $\xi \sim \mathcal{N}(0, I)$ and [2]

$$\begin{aligned} \alpha^2 + \delta^2 &= \sigma^2\left(t - 2(n+1)\tau\left(1 - e^{-\frac{t}{(n+1)\tau}}\right) + \frac{(n+1)\tau}{2}\left(1 - e^{-\frac{2t}{(n+1)\tau}}\right)\right), \\ \beta\alpha &= \frac{\sigma^2\sqrt{\tau}(n+1)}{2}\left[1 - e^{-\frac{t}{(n+1)\tau}}\right]^2, \\ \beta^2 &= \frac{(n+1)\sigma^2}{2}\left[1 - e^{-\frac{2t}{(n+1)\tau}}\right]. \end{aligned} \tag{2.18}$$

The split-step approximation for inertial particles is given by

$$\begin{pmatrix} x_{k+1} \\ y_{k+1}\end{pmatrix} = \widehat{\psi}(x_k, y_k, \Delta t, \xi, \gamma), \tag{2.19}$$

where

$$\widehat{\psi}(x,y,t,\xi,\gamma) = \lambda \circ \hat{\phi}(x,y,t) + g(\xi,\gamma,t). \tag{2.20}$$

[2] For details on how to calculate α, β, δ, see Appendix D.

Before we proceed to the next section we briefly discuss how we solve (2.14). The integrals in (2.14) can be calculated with some high level quadrature. However, we take advantage of the fact that we can substitute for $y^j(t)$ in the $x^j(t)$ equation and convert the double integral into a single integral to obtain

$$\begin{aligned} x^j(t) &= x^j(0) + \sqrt{\tau}y^j(0)\left(1 - \exp\left[-\frac{t}{(n+1)\tau}\right]\right) + \int_0^t \left(1 - \exp\left[-\frac{(t-s)}{(n+1)\tau}\right]\right) f_j(s)ds, \\ y^j(t) &= y^j(0)\exp\left[-\frac{t}{(n+1)\tau}\right] + \frac{1}{\sqrt{\tau}}\int_0^t \exp\left[-\frac{(t-s)}{(n+1)\tau}\right] f_j(s)ds. \end{aligned} \tag{2.21}$$

In order to calculate the convolution integral arising in both cases we make the substitution $q = e^{\frac{s}{(n+1)\tau}}$ to obtain

$$\int_0^t \exp\left[-\frac{(t-s)}{(n+1)\tau}\right] f_j(s)ds = (n+1)\tau e^{-\frac{t}{(n+1)\tau}} \int_1^{e^{\frac{t}{(n+1)\tau}}} d_j v_j\left(a - \frac{b(n+1)\tau}{q}\right)dq.$$

We now approximate the integral on the right-hand side by a simple Euler method to obtain

$$e^{-\frac{t}{(n+1)\tau}} \int_1^{e^{\frac{t}{(n+1)\tau}}} d_j v_j\left(a - \frac{b(n+1)\tau}{q}\right)dq \approx \left(1 - e^{-\frac{t}{(n+1)\tau}}\right) d_j v_j(a - b\tau(n+1)),$$

where

$$\left(1 - e^{-\frac{t}{(n+1)\tau}}\right) d_j v_j(a - b\tau(n+1)) = \left(1 - e^{-\frac{t}{(n+1)\tau}}\right) d_j v_j(\langle e_j, x^j(0)\rangle),$$

while the other integral in the x equation in (2.21) is approximated using the trapezoid rule. Thus we obtain the following approximation to $\widehat{\phi}_j(x,y,t)$, denoted by $\tilde{\phi}_j(x,y,t)$, where

$$\tilde{\phi}_j(x,y,t) = \lambda(x,y,t) + \mu_j(x,y,t),$$

and

$$\mu_j(x,y,t) = \begin{pmatrix} (n+1)\tau\left(1 - e^{-\frac{t}{(n+1)\tau}}\right) d_j v_j(\langle e_j, x\rangle) + h_j(x,y,t) \\ (n+1)\sqrt{\tau}\left(1 - e^{-\frac{t}{(n+1)\tau}}\right) d_j v_j(\langle e_j, x\rangle) \end{pmatrix},$$

with

$$h_j(x,y,t) = d_j \frac{t}{2}\left[v_j(\langle e_j, x\rangle) + v_j\left(\left\langle e_j, x + \left(1 - e^{-\frac{t}{(n+1)\tau}}\right)y\right\rangle\right)\right].$$

We find this effective in practice, especially for small τ.

3. Analysis of the numerical method

3.1. Convergence of the stochastic splitting method

In this subsection we present a result regarding the strong order of convergence for the stochastic splitting methods. Note that we can write (1.1) and (1.4) as a system of first-order SDE's namely:

$$\dot{z} = F(z) + \Sigma\dot{W}, \tag{3.1}$$

where $z \in \mathbb{R}^l$ and $l = d$ or $l = 2d$, $F(z) = \sum_1^n F_i(z)$, and $\Sigma \in \mathbb{R}^{l\times d}$ and W is an d-dimensional standard Brownian motion. We now state and prove a theorem concerning the convergence of the numerical method.

Theorem 1. *Let x_k be the numerical approximation of (3.1) by the stochastic splitting method at time $k\Delta t$, where $F(x) = \sum_{i=1}^n F_i(x)$, $F_j \in C^2(\mathbb{R}^l, \mathbb{R}^l)$. Suppose that*

$$\mathbb{E}(|x_0|^2) < \infty, \tag{3.2a}$$

$$\mathbb{E}(|x_0 - y_0^{\Delta t}|^2)^{1/2} \le K_1 \Delta t^{1/2}, \tag{3.2b}$$

$$|F_j(x) - F_j(y)| \le K_2|x - y|, \quad j = 1, \ldots, n, \tag{3.2c}$$

where the constant K_1, K_2 do not depend on Δt. Then

$$\left(\mathbb{E}\sup_{0\le k\Delta t\le T} |x(k\Delta t) - x_k|^2\right)^{1/2} \le C_2(T)\Delta t \quad \forall T > 0. \tag{3.3}$$

Proof 1. Let $\widehat{y}_k$ be the approximation of (3.1) by the Euler–Maryama method at time $k\Delta t$. The following result holds, when the assumptions of Theorem 1 hold [11]:

$$\left(\mathbb{E}\sup_{0\le k\Delta t\le T}|x(k\Delta t)-\widehat{y}_k|^2\right)^{1/2}\le C(T)\Delta t. \tag{3.4}$$

Thus, using the triangle inequality:

$$\left(\mathbb{E}\sup_{0\le k\Delta t\le T}|x(k\Delta t)-x_k|^2\right)^{1/2}\le\left(\mathbb{E}\sup_{0\le k\Delta t\le T}|x(k\Delta t)-\widehat{y}_k|^2\right)^{1/2}+\left(\mathbb{E}\sup_{0\le k\Delta t\le T}|\widehat{y}_k-x_k|^2\right)^{1/2}.$$

Using Lemma 14 from the Appendix C and Eq. (3.4) we obtain

$$\left(\mathbb{E}\sup_{0\le k\Delta t\le T}|x(k\Delta t)-x_k|^2\right)^{1/2}\le C_2(T)\Delta t. \qquad \square$$

Note that the strong order of convergence is 1, as in the case of the Euler–Marayama method with additive noise [11].

3.2. Splitting method in the case of small inertia

In this subsection we investigate the behaviour of the stochastic splitting method in the case of small inertia. Our interest is in studying the behaviour of the method as $\tau\to 0$. When we send τ to 0, while keeping Δt fixed, we recover the solution of the splitting method for the passive tracers problem. This is the content of the following theorem.

Theorem 2. *Let $x_{\Delta t}(T)$, $x^{\tau}_{\Delta t}(T)$ denote the numerical approximations to Eqs. (1.1) and (1.4) obtained at time $T=n\Delta t$ using the stochastic splitting method. Let the assumptions of Theorem 1 hold. Then:*

$$\left(\mathbb{E}(\|x_{\Delta t}(T)-x^{\tau}_{\Delta t}(T)\|^2)\right)^{1/2}\le C(T)\frac{\sqrt{\tau}}{\Delta t}. \tag{3.5}$$

Proof 2. We need to introduce the operators P_x and P_y

$$P_x\begin{pmatrix}x\\y\end{pmatrix}=x,\quad P_y\begin{pmatrix}x\\y\end{pmatrix}=y,$$

where $x,y\in\mathbb{R}^d$. In Section 3 we defined the maps $\widehat{\psi}(x,y,\Delta t,\gamma,\xi),\ \psi(x,\Delta t,\gamma)$ and expressed the numerical solution for both passive tracers and inertial particles through

$$\text{passive tracers},\quad x_{k+1}=\psi(x_k,\Delta t,\gamma_k),$$
$$\text{inertial particles},\quad (\widehat{x}_{k+1},\widehat{y}_{k+1})=\widehat{\psi}(\widehat{x}_k,\widehat{y}_k,\Delta t,\xi_k,\gamma_k).$$

We now set $e_k=\widehat{x}_k-x_k$ to obtain

$$\begin{aligned}e_{k+1}&=P_x\widehat{\psi}(\widehat{x}_k,\widehat{y}_k,\Delta t,\gamma_k,\xi_k)-\psi(x_k,\Delta t,\gamma_k)=P_x(\lambda\circ\widehat{\phi})(\widehat{x}_k,\widehat{y}_k,\Delta t)+P_xg(\xi_k,\gamma_k,\Delta t)-\phi(x_k,\Delta t)-\sigma\sqrt{\Delta t}\gamma_k\\&=P_x\widehat{\phi}(\widehat{x}_k,\widehat{y}_k,\Delta t)+\sqrt{\tau}P_y\left[1-\exp\left(-\frac{\Delta t}{(n+1)\tau}\right)\right]\widehat{\phi}(\widehat{x}_k,\widehat{y}_k,\Delta t)-\phi(x_k,\Delta t)+P_xg(\xi_k,\gamma_k,\Delta t)-\sigma\sqrt{\Delta t}\gamma_k.\end{aligned}$$

We take norms and use the triangle inequality to obtain

$$\|e_{k+1}\|\le\|P_x\widehat{\phi}(\widehat{x}_k,\widehat{y}_k,\Delta t,)-\phi(x_k,\Delta t)\|+\sqrt{\tau}\|P_y\widehat{\phi}(\widehat{x}_k,\widehat{y}_k,\Delta t)\|+\|P_xg_k(\gamma_k,\xi_k,\Delta t)-\sigma\sqrt{\Delta t}\xi_k\|.$$

Using Lemma 12 from Appendix B we obtain

$$\|e_{k+1}\|\le(1+K\Delta t)\|e_k\|+C\sqrt{\tau}+\|P_xg_k(\gamma_k,\xi_k,\Delta t)-\sigma\sqrt{\Delta t}\gamma_k\|, \tag{3.6}$$

and if we take expectations and use Lemma 13 from the Appendix B, together with Jensen's inequality for the noisy part we conclude

$$\mathbb{E}(\|e_{k+1}\|)\le(1+K\Delta t)\mathbb{E}(\|e_k\|)+(M+C)\sqrt{\tau}.$$

We now use the discrete Gronwall inequality and set $C_1=M+C$ to obtain

$$\mathbb{E}(\|e_k\|)\le\left(\frac{(1+K\Delta t)^k-1}{(1+K\Delta)-1}C_1\tau\right)\le(e^{kT}-1)\frac{C_1\sqrt{\tau}}{K\Delta t},$$

since $(1+L\Delta t)^n\le e^{nL\Delta t}$. Hence we deduce that

$$\mathbb{E}(\|e_k\|) \le C_1 e^{kK\Delta t}\frac{\sqrt{\tau}}{\Delta t}. \tag{3.7}$$

We now use (3.6) again by taking squares and then expectations to obtain

$$\mathbb{E}(\|e_{k+1}\|^2) \le (1+K\Delta t)^2\mathbb{E}(\|e_k\|^2) + C^2\tau + 4\left[C\sqrt{\tau} + \mathbb{E}(\|P_x g(\xi_k,\gamma_k,\Delta t) - \sigma\Delta t\gamma_k\|)\right]\mathbb{E}(\|e_k\|) + 2C\sqrt{\tau}\mathbb{E}(\|P_x g(\xi_k,\gamma_k,\Delta t) - \sigma\Delta t\gamma_k\|) + \mathbb{E}(\|P_x g(\xi_k,\gamma_k,\Delta t) - \sigma\Delta t\gamma_k\|^2),$$

where in the second line we have used the fact that $K\Delta t \le 1$. We can now use Eq. (3.7) together with Lemma 13 from Appendix B to obtain

$$\mathbb{E}(\|e_{k+1}\|^2) \le (1+L\Delta t)\mathbb{E}(\|e_k\|^2) + M\tau + C_1 e^{KT}\frac{\tau}{\Delta t}.$$

By applying the discrete Gronwall inequality we conclude that

$$(\mathbb{E}(\|x_{\Delta t}(T) - x^{\tau}_{\Delta t}(T)\|^2))^{1/2} \le C(T)\frac{\sqrt{\tau}}{\Delta t}. \qquad \square$$

4. Relevant asymptotics limits

In this section we present various results for different asymptotic limits of interest. These results are presented here purely for the purpose of guiding our numerical experiments and thus no proofs are given. We start by presenting results concerning the vanishing molecular diffusion limit of the Taylor–Green velocity field and the shear flow in the passive tracers model (1.1). We also present a result regarding the effective diffusive behaviour of passive tracers driven by colored noise.

We then present results for inertial particles, giving a new bound for the effective diffusivity of inertial particles for the shear flow. The case of small inertia is also studied and a result is then presented for the relation between the effective diffusivity of inertial particles for small inertia and the effective diffusivity of passive tracers. Finally, in the last subsection we present a modified passive tracers model obtained from averaging the inertial particles model in the case $\sigma = \sqrt{\tau}$ and $\tau \ll 1$. Throughout this section we use the following definition for the effective diffusivity.

Definition 3. The effective diffusivity matrix is defined (when it exists) as

$$\mathcal{K} = \lim_{t\to\infty}\frac{\langle (x(t)-x(0))\otimes(x(t)-x(0))\rangle}{2t}, \tag{4.1}$$

where $x(t)$ is the solution of the equations of motion (i.e. (1.1), (1.2) or (1.4)) and $\langle\cdot\rangle$ denotes ensemble average.

It is possible to prove rigorously for all the problems that we consider in this paper, namely Eqs. (1.1), (1.2), (1.4) with time independent, periodic and incompressible velocity fields, that the effective diffusivity exists. More precisely, the rescaled process

$$x^{\epsilon}(t) := \epsilon x(t/\epsilon^2),$$

where $x(t)$ is the solution of the equations of motion, converges weakly (as a probability measure over the space of continuous functions on $\mathbb{R}^d$) to a Brownian motion $W(t)$ with covariance matrix $\mathcal{K}$:

$$x^{\epsilon}(t) \Rightarrow \sqrt{2\mathcal{K}}W(t). \tag{4.2}$$

4.1. Passive tracers

In this subsection we present results regarding passive tracers in the limit of vanishing molecular diffusion, together with a result concerning passive tracers driven by colored noise.

4.1.1. The small molecular diffusion limit

We now describe two results concerning the behaviour of the effective diffusivity in the vanishing molecular diffusion limit for the passive tracers. We study both the Taylor–Green velocity field and the shear flow.

Taylor–Green velocity field

Result 4 [8,9,13]. Let $x(t)$ be the solution of the passive tracers with $v(x)$ given by Eq. (2.1). Then the following results holds in the case $\sigma \ll 1$:

$$\mathcal{K}(\sigma) \sim \sigma I_2,$$

where I_2 is the two-dimensional unit matrix.

Note that in the case where $v(x) = 0$, the effective diffusivity matrix is

$$\mathcal{K}(\sigma) = \frac{\sigma^2}{2} I_2.$$

Thus the relative enhancement of the effective diffusivity for the Taylor–Green field over the bare molecular diffusivity is unbounded in the limit $\sigma \to 0$.

The convergence result (4.2) does not provide us with any information concerning the relevant time scales, in particular the time needed for the systems to reach the asymptotic regime which can be described through an effective Brownian motion. The scaling of the *diffusive time* t_{diff} with respect to the molecular diffusivity σ was studied in [8] for various types of incompressible flows, for the passive tracers problem.

Result 5 [8]. Let $x(t)$ be the solution of passive tracers with $v(x)$ given by Eq. (2.1) and t_{diff} be the time it takes for the particle to start behaving diffusively. Then

$$t_{diff} \sim \frac{1}{\sigma^2}, \quad \sigma \ll 1.$$

Shear flow

Another flow of interest is the shear flow

$$v(x) = \begin{pmatrix} 0 \\ \sin x_1 \end{pmatrix}. \tag{4.3}$$

For this flow an explicit calculation gives the following result:

Result 6 [13,22]. Let $x(t)$ be the solution of passive tracers with $v(x)$ given by Eq. (4.3). Then the effective diffusivity matrix is given by

$$\mathcal{K}(\sigma) = \begin{pmatrix} \frac{\sigma^2}{2} & 0 \\ 0 & \frac{\sigma^2}{2} + \frac{1}{\sigma^2} \end{pmatrix}. \tag{4.4}$$

Note that the result shows that the effective diffusivity is unbounded, in absolute terms, in the second component of the system as $\sigma \to 0$. This remarkable effect arises from ballistic transport over long distances, slowly modulated by molecular diffusion.

4.1.2. Passive tracers driven by colored noise

In various applications it is sometimes of interest to consider passive tracers driven by coloured noise (see [4] and references within). The equations of motion are then

$$\dot{x} = v(x) + \frac{\sigma\eta}{\sqrt{\delta}}, \tag{4.5a}$$

$$\dot{\eta} = -\frac{\eta}{\delta} + \frac{1}{\sqrt{\delta}}\dot{W}. \tag{4.5b}$$

Techniques from homogenization show that Eq. (1.1) is recovered in the limit $\delta \to 0$ [22].

It can be proven then, that under appropriate assumptions on the velocity field, the effective behaviour of x satisfying (4.5), is governed by a Brownian motion with an effective diffusivity matrix $\mathcal{K}(\sigma, \delta)$. For the derivation of the effective equation using the backward Kolmogorov equation for such systems we refer to [38], while the same derivation from the point of view of the Fokker–Planck equation can be found in [4]. The following result describes the limit $\delta \to 0$.

Result 7 [38]. Let $\mathcal{K}(\sigma, \delta)$ be the effective diffusivity matrix for $x(t)$ governed by (4.5) and $\mathcal{K}(\sigma)$ the effective diffusivity matrix for $x(t)$ governed by (1.1). Then, for σ fixed and $\delta \ll 1$,

$$\mathcal{K}(\sigma, \delta) = \mathcal{K}(\sigma) + C(\sigma)\delta + \mathcal{O}(\delta^{3/2}). \tag{4.6}$$

4.2. Inertial particles

In this subsection we present some relevant results for inertial particles.

4.2.1. Shear flow

We can use Result 6 to deduce the following result for inertial particles:

Result 8 [38]. Let $x(t)$ be the solution of (1.4) with $v(x)$ given by (4.3). Then the effective diffusivity matrix is given by

$$\mathcal{K}(\sigma, \tau) = \begin{pmatrix} \frac{\sigma^2}{2} & 0 \\ 0 & \mathcal{K}_{22}(\sigma, \tau) \end{pmatrix},$$

where for some C_1, C_2 independent of σ and τ,

$$|\mathcal{K}_{22}(\sigma,\tau) - \mathcal{K}_{22}(\sigma)| \leq \frac{2C_1}{\sigma} + C_2\tau. \tag{4.7}$$

Here, $\mathcal{K}_{22}(\sigma)$ is given by (4.4) as

$$\mathcal{K}_{22}(\sigma) = \frac{\sigma^2}{2} + \frac{1}{\sigma^2}.$$

Note that Eq. (4.7) shows that for $\sigma \ll 1$ and $\tau = \mathcal{O}(1)$, $\mathcal{K}_{22}(\sigma,\tau)$ behaves like $\mathcal{K}_{22}(\sigma)$, since in this case $\mathcal{K}_{22}(\sigma)$ grows like $1/\sigma^2$. This explains the numerical results in [23], where it was shown that $\mathcal{K}$ is effectively independent of τ in the inertial particles case.

4.2.2. The case of small inertia

In this subsection we study the case of small inertia. We have the following theorem, using techniques from [24]

Theorem 9 [38]. *Let x, x^τ solve the stochastic differential equations*

$$\dot{x} = v(x) + \sigma\dot{W}, \tag{4.8a}$$

$$\tau\ddot{x}^\tau = v(x^\tau) - \dot{x}^\tau + \sigma\dot{W}, \tag{4.8b}$$

where $v \in C(\mathbb{T}^d, \mathbb{R}^d)$. Then

$$\left(\mathbb{E}\sup_{0\leq t\leq T}\|x^\tau(t) - x(t)^2\right)^{1/2} \leq K\sqrt{\tau\log\left(\frac{T}{\tau}+2\right)}e^{LT}.$$

Proof 3. This theorem is proved using techniques applied to the more general problem considered in [24].

Theorem 9 gives us only pathwise information, but it does not reveal the relation between the effective diffusivity of inertial particles and passive tracers in the small inertia limit. The following result relates the effective diffusivity of passive tracers with the one of inertial particles in the small τ regime:

Result 10 [25]. Let $\mathcal{K}(\sigma,\tau)$ be the effective diffusivity matrix for $x(t)$ governed by (1.4) and $\mathcal{K}(\sigma)$ the effective diffusivity matrix for $x(t)$ governed by (1.1). Furthermore, assume that $\nabla\cdot v = 0$. Then for σ fixed and $\tau \ll 1$,

$$\mathcal{K}(\sigma,\tau) = \mathcal{K}(\sigma) + \mathcal{O}(\sqrt{\tau}).$$

4.2.3. The case $\sigma = \sqrt{\tau}$

We now present a result for the case where $\sigma = \sqrt{\tau}$ and $\tau \to 0$ using formal asymptotics arguments. It is exactly this relationship between σ, τ that makes such a treatment possible, since then the leading order operator is ergodic and thus we can apply the techniques of stochastic averaging.

The next result follows from formal perturbation arguments, similar to those used in Part II of [22]; details are given in Appendix A.

Result 11. For $\tau \ll 1$ and $t = \mathcal{O}(1)$ the dynamics of the inertial particles model

$$\tau\ddot{x}^\tau = v(x) - \dot{x}^\tau + \sqrt{\tau}\dot{W}, \tag{4.9}$$

are approximated by the modified passive tracers model

$$\dot{x} = v(x) - \tau(\nabla v(x))v(x) + \sqrt{\tau}\dot{W}. \tag{4.10}$$

In the case $\tau = 0$ the modified passive tracers model is simply the equation for Langrangian trajectories, while in the absence of Brownian motion it is precisely the two-term approximation of the invariant manifold found in [29].

5. Numerical investigations: the vanishing molecular diffusion limit

In this section we investigate the performance of the stochastic splitting method in the vanishing molecular diffusion limit. We study its behaviour for both passive tracers and inertial particles; and we use both the Taylor–Green velocity field and the shear flow. The objectives of our investigation in this section are as follows:

(i) To compare the stochastic splitting method with the Euler method in the passive tracers and the inertial particles case.
(ii) To use modified equations to show that the Euler method is not suitable for the passive tracers case.
(iii) To apply the stochastic splitting method in a slightly different setting, the case of passive tracers driven by colored noise, thereby obtaining new information about this problem.

(iv) To numerically illustrate Result 8 regarding the behaviour of the effective diffusivity of the inertial particles moving in the shear flow.
(v) To obtain new results for the vanishing molecular diffusion limit in the case of inertial particles.

5.1. Passive tracers

In this subsection we study the behaviour of the stochastic splitting method in the vanishing molecular diffusion limit for passive tracers. Note that the behaviour of the effective diffusivity is analytically known for the shear flow (Result 6) and the Taylor–Green velocity field (Result 4). This provides us with a good testing ground for the stochastic splitting method. Note that in the case of shear flow the Euler method and the stochastic splitting method are the same and thus we do not present any results for the shear flow in the case of passive tracers.

We now present some numerical results concerning the passive tracers problem as $\sigma \to 0$ for the Taylor–Green velocity field. In this case the effective diffusivity matrix is diagonal with the diagonal elements scaling like σ.

In Fig. 1 we plot the phase plane of (1.1) for $\sigma = 10^{-2}$ with the use of the two different numerical methods. The realization of the noise is the same for the two methods and we have integrated up to time $T = 10^4$ with timestep $\Delta t = 10^{-2}$.

It is clear that the behaviour of the particle is drastically different. In the case of the Euler–Maryama method the particle appears to be much more diffusive than in the case of the stochastic splitting method.

We now compare the two methods in the case of zero noise, since that will help us to understand the different behaviour in the small noise regime. In Fig. 2 we draw the phase plane in the absence of noise.

In the absence of noise the system is autonomous Hamiltonian, and hence volume-preserving. The stochastic splitting method inherits the property of being volume-preserving in the absence of noise, whilst the Euler method does not. This difference is manifested in Fig. 2 where, in the absence of noise, the Euler method leads to solutions which spiral out, whilst the splitting method leads to closed orbits. When σ is small the spiraling effect in the Euler method leads to faster escapes from the cell than the stochastic splitting method and hence to overestimated effective diffusivities.

In Fig. 3 we plot $\mathcal{K}_{11}$ as a function of the molecular diffusivity σ for the two different methods. For both of the methods we have used $N = 10^3$ realizations integrating up to $T = 10^5$ with time step $\Delta t = 10^{-2}$. We can clearly see that for large values of molecular diffusivity the two methods agree, but as σ gets smaller the Euler method fails to capture the results predicted by theory. The stochastic splitting method, however, agrees with the theory. If we fit our data for values of $\sigma \in [5 \times 10^{-3}, 10^{-1}]$, we find that the effective diffusivity grows like $c^*\sigma^a$, where $a = 1.0946,\ c^* = 1.0575$, while the theory predicts that $a = 1.0$.

We now reduce the time step to $\Delta t = 5 \times 10^{-3}$ to obtain Fig. 4 and consider only the stochastic splitting method. We can clearly see that the numerical results agree almost perfectly with the theory for $\sigma \in [5 \times 10^{-2}, 5 \times 10^{-1}]$. If we now fit the data for $\sigma \in [5 \times 10^{-3}, 10^{-1}]$, we find that the effective diffusivity grows like $c^*\sigma^a$, where $a = 1.0579,\ c^* = 0.9269$, which agrees almost perfectly with the theory.

For values of σ smaller than 5×10^{-3}, we see that the effective diffusivity does not behave as the theory predicts, even for the splitting method. However, this should not come as a surprise, since as we see in Result 5 the time for the particle to be diffusive is of order $1/\sigma^2$ and thus integrating up to $T = 10^5$ is not enough, since the particle has not yet reached its diffusive regime.

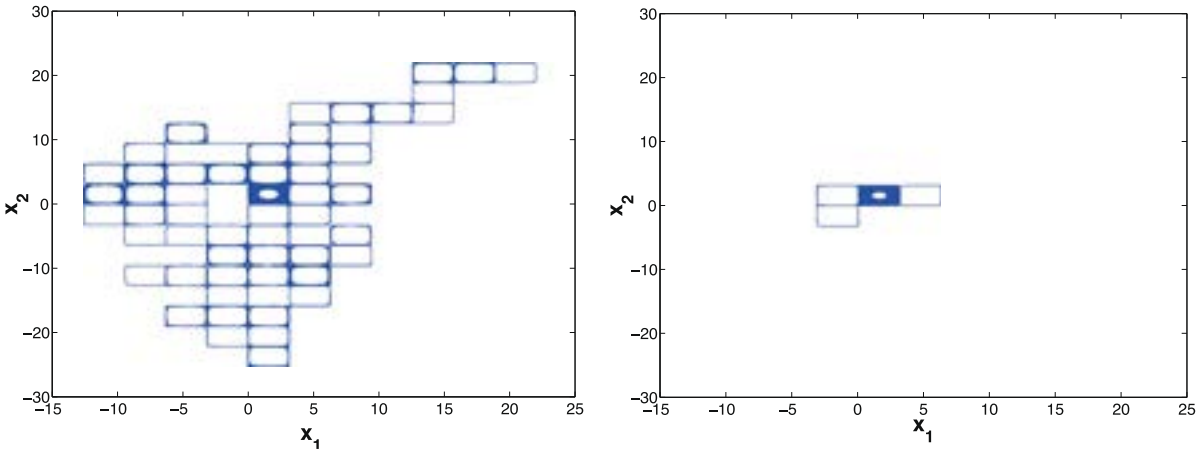

(a) Euler method. (b) Stochastic splitting method.

Fig. 1. Phase plane for the two different methods.

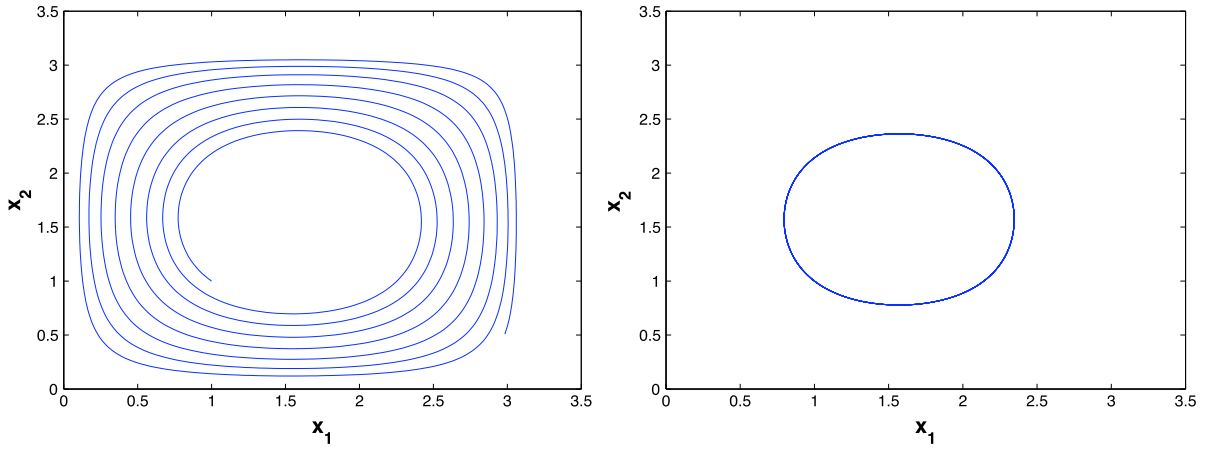

(a) Euler method. (b) Stochastic splitting method.

Fig. 2. Phase plane for the two different methods in the absence of noise.

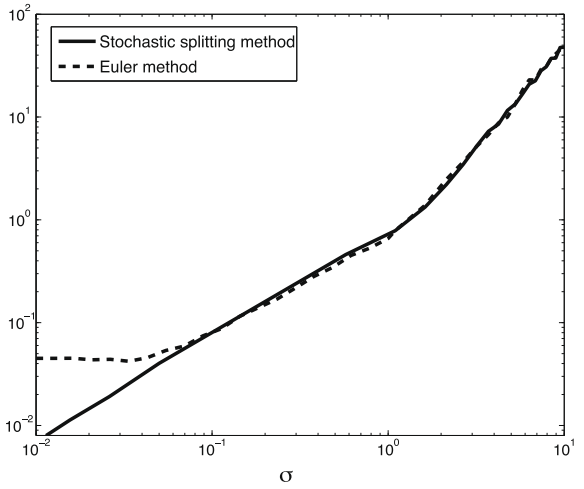

Fig. 3. Effective diffusivity as a function of σ for the two different methods.

Before rejecting the Euler–Maryama method for our problem we will make one last comparison. We expect that the volume preserving method is roughly three times slower than the Euler method, since it involves two extra steps in order to compute the value of the solution at each timestep. Thus, a fair comparison is to compare the Euler method over the splitting method, when the former uses a timestep that is one-third of the latter. So, we use a timestep of $\Delta t = 10^{-1}$ for the volume preserving method and then calculate the effective diffusivity for $\sigma = 10^{-2}$ using $N = 10^3$ trajectories. We repeat the calculation with the Euler method. We then decrease the timestep by successive factors of two until our final timestep becomes $\Delta t = 10^{-1}/2^4$. The results are plotted in Fig. 5.

The failure of the Euler method is once again obvious. Even when we use the a timestep 16 times smaller than the one used in the splitting method, the calculated effective diffusivity is 5 times larger than the correct value, which is reproduced by the splitting method.

The Euler method not only forces the particle to behave more diffusively but also to reach its diffusive regime much faster than the theory predicts. This is clearly exhibited in Fig. 6, where we plot the effective diffusivity as a function of time. We know from Result 5 that the time it takes for the particle to start behaving diffusively is $\mathcal{O}(1/\sigma^2)$. This order of magnitude is indicated by the vertical line in Fig. 6. The first line from the top corresponds to the Euler–Maryama method for $\Delta t = 10^{-1}/4$ and the two below for $\Delta t = 10^{-1}/8$, $\Delta t = 10^{-1}/16$, while the last line corresponds to the stochastic splitting method for $\Delta t = 10^{-1}$. It is clear that the particle reaches its diffusive regime faster than it should when the Euler–Maryama method is used.

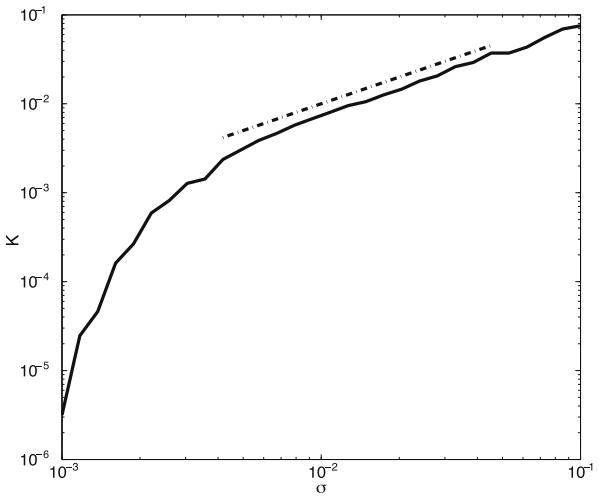

Fig. 4. Effective diffusivity for $\sigma \ll 1$ using the stochastic splitting method.

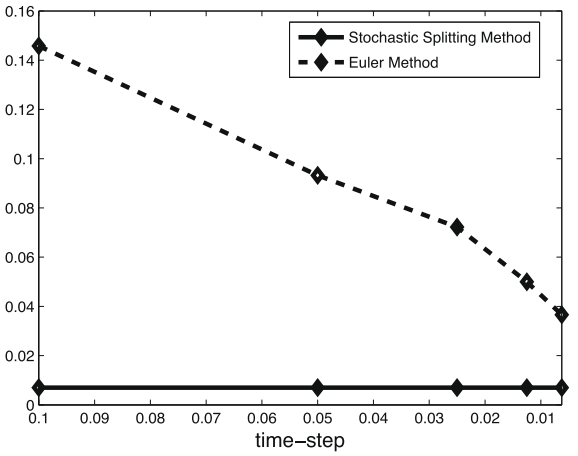

Fig. 5. Comparison of the two methods for $\sigma = 0.01$ and different timesteps.

5.2. Modified equations

In this subsection we study the Euler method with the use of modified equations. Modified equations is a widely used method for backward error analysis [10] for ordinary differential equations. In the case of stochastic differential equations the derivation of modified equations is more complicated, because the semigroup governing the expectation propagation is not invertible. However, some limited work is available and we employ a form of weak backward error analysis from [30].

Consider the following SDE

$$dX = f(X)dt + \sigma(X)dW(t), \quad X(0) = Y, \tag{5.1}$$

where $X \in \mathbb{R}^d$ and W a d-dimensional standard Brownian motion. Let us consider a numerical approximation $X_0, X_1, \ldots, X_n$ of weak order 1

$$|\mathbb{E}\phi(X_n) - \mathbb{E}\phi(X(n\Delta t))| = \mathcal{O}(\Delta t), \quad 0 \le n\Delta t \le T \tag{5.2}$$

for ϕ in a space of smooth test functions [11]. We would like to modify the SDE (5.1) to define a process $\widetilde{X}$ that better describes the numerical approximation X_n, in the sense that

$$|\mathbb{E}\phi(X_n) - \mathbb{E}\phi(\widetilde{X}(n\Delta t))| = \mathcal{O}(\Delta t^2), \quad 0 \le n\Delta t \le T.$$

We define $\widetilde{X}$ as the solution to the modified SDE

$$d\widetilde{X} = [f(\widetilde{X} + \tilde{f}(\widetilde{X}))\Delta t]dt + [\sigma(\widetilde{X}) + \tilde{\sigma}(\widetilde{X})\Delta t]dW(t), \quad \widetilde{X}(0) = Y, \tag{5.3}$$

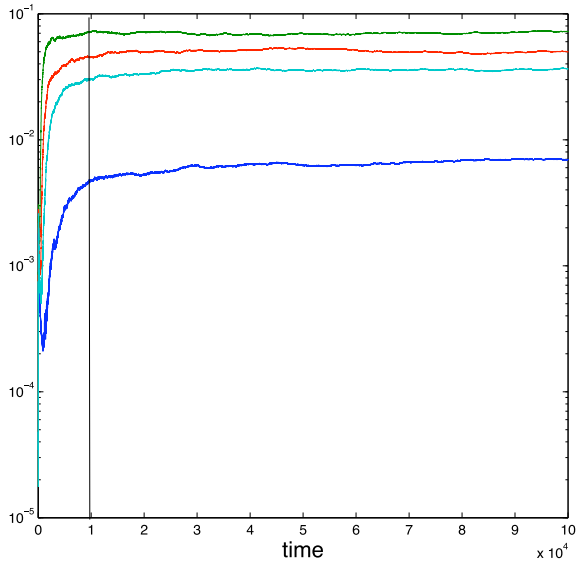

Fig. 6. $\frac{\langle (x_1(t)-x_1(0))^2\rangle}{2t}$ as a function of time for the two different methods.

where $\tilde{f}, \tilde{\sigma}$ are smooth functions to be determined. In [30] $\tilde{f}, \tilde{\sigma}$ were derived in the case of the Euler method with additive noise. For our Eq. (4.8a) the modified equation is

$$\dot{x} = \left(v(x) - \frac{\Delta t}{2} (\nabla v(x)) v(x) - \frac{\sigma^2 \Delta t}{4} \Delta v(x) \right) dt + \sigma \left(1 - \frac{\Delta t}{2} \nabla v^T(x) \right) \dot{W}. \tag{5.4}$$

Note that the correction proportional to $\sigma^2 \Delta t$ in the drift is related to the presence of noise in the problem, since in the absence of noise the modified equation for the Euler method would only contain the $(\nabla v(x))v(x)$ correction [10].

If $v = \nabla^{\perp} \Psi$ we apply Itô's formula to the stream function $\Psi(x)$ for x satisfying (1.1), to find

$$\dot{\Psi} = \frac{\sigma^2}{2} \Delta \Psi + M. \tag{5.5}$$

Here the integral of M is a mean zero martingale.

In the case of the Taylor–Green flow $\Delta \Psi = -2\Psi$, so Eq. (5.5) becomes

$$\dot{\Psi} = -\sigma^2 \Psi + M. \tag{5.6}$$

Thus the mean value of the stream function decays like e^{-t/σ^2}. We now apply Itô's formula to the stream function $\Psi(x)$ for the Taylor–Green flow for x satisfying the modified equation (5.4). We find that

$$\frac{d\Psi}{dt} = -\frac{\Delta t}{2} (\cos^2 x_1 + \cos^2 x_2) \Psi - \sigma^2 \Psi (1 + \Delta t \cos x_1 \cos x_2) + \frac{\sigma^2 \Delta^2 t}{4} (\cos^2 x_1 \cos^2 x_2 \Psi - \Psi^3) + M_{\Delta t}, \tag{5.7}$$

where the integral of $M_{\Delta t}$ is again a mean zero martingale.

Note that in the case $\Delta t = 0$, Eq. (5.7) becomes (5.6). However, the first term on the right-hand side of (5.7) does not depend on σ. When $\Delta t \gg \mathcal{O}(\sigma^2)$ this term causes the spiraling effect seen in Fig. 2a. Furthermore, it drastically changes the behaviour of the mean value of the Hamiltonian Ψ as a function of time as seen in Fig. 7, where the mean value of the Hamiltonian as a function of time is plotted for the two different methods, together with the real solution. As we can see, in the case of the Euler method the mean Hamiltonian decays much faster than the theory predicts, while in the case of the stochastic splitting method it decays at the right rate.

5.3. Passive tracers driven by coloured noise

In this section we study numerically the motion of passive tracers in the Taylor–Green velocity field subject to coloured noise, using a generalization of the stochastic splitting method. More precisely, the deterministic steps are the same as in the case of passive tracers driven by white noise. However, when we add the noise, instead of just adding white noise, we add an exactly sampled integral of the OU process. This is achieved using similar techniques to those employed in the limit of small τ for inertial particles.

In Fig. 8 we plot the effective diffusivity as a function of σ for $\delta = 10^{-1}$, and $\delta = 1$ for the two different methods. In our calculations we have used a time step $\Delta t = 10^{-2}$, with final integration time $T = 10^5$ for $N = 10^3$ paths.

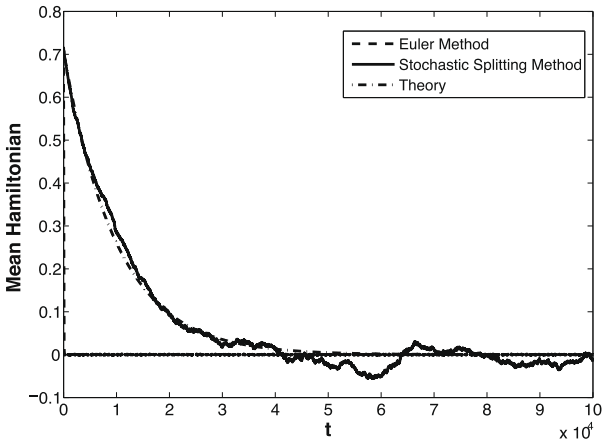

Fig. 7. Mean value of the Hamiltonian as a function of time, for $\Delta t = 10^{-1}$, $\sigma = 10^{-2}$.

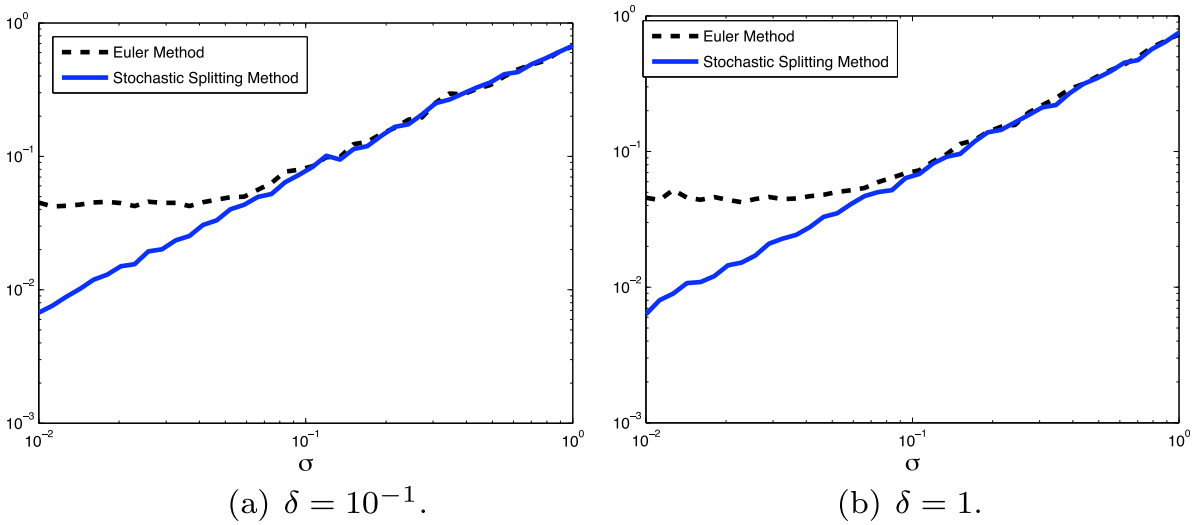

Fig. 8. Effective diffusivity as a function of σ for the two different methods.

In the case of $\delta = 10^{-1}$ we expect that the effective diffusivity for the coloured problem should be close to the one of the white problem (Result 7) and thus it should go to zero as $\sigma \to 0$. As we can see this is the case for the stochastic splitting method, but not for the Euler method. This should not be a surprise, since as we have already seen in the case of white noise the Euler method does not capture the right behaviour for the effective diffusivity. Similar behaviour is observed for $\delta = 1$. In particular, the numerical experiments suggest that the effective diffusivity when $\sigma \ll 1$ is essentially independent of δ.

5.4. Inertial particles

In this subsection we study the performance of the stochastic splitting method for the case of inertial particles, and we also study the dependence of the effective diffusivity on the various parameters of the problem. We study both the shear flow and the Taylor–Green velocity field. In doing this we should keep in mind that the behaviour of the effective diffusivity is known for the shear flow (Result 8), but not for the Taylor–Green velocity field.

5.4.1. Shear flow

We now present some numerical results concerning the inertial particles problem in the vanishing molecular diffusion limit for the shear flow. Note that, in contrast to the passive tracers, the Euler and the stochastic splitting method differ in the inertial case. In Result 8 we have shown that in the vanishing molecular diffusion limit the $\mathcal{K}_{22}$ element of the matrix diverges like $1/\sigma^2$. Thus, this is the scaling that we expect our method to capture as $\sigma \to 0$ for τ of $\mathcal{O}(1)$.

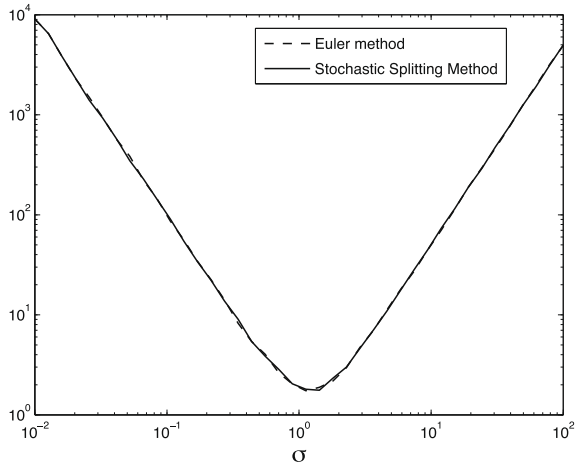

Fig. 9. Effective diffusivity as a function of σ for the two different methods for the shear flow.

We now start our investigation by computing effective diffusivities with the two different methods. In Fig. 9 we compare the effective diffusivities for the two different methods. For this figure the time step used was $\Delta t = 10^{-3}$ and we integrated for time $T = 10^5$, using $N = 10^3$ realizations. If we now try to fit the data for $\sigma \in [10^{-2}, 5 \times 10^{-1}]$, we find that the effective diffusivity behaves like $b\sigma^a$ where $b = 1.077,\ a = -1.9665$ for the stochastic splitting method and $b = 1.0892,\ a = -1.9706$ for the Euler method and both of them agree with what is predicted by Result 8.

5.4.2. Taylor–Green velocity field

We now present some numerical results concerning the inertial particles problem for the Taylor–Green flow in the limit of vanishing molecular diffusion.

Note that in this case no analytical result for the behaviour of the effective diffusivity is known, in contrast with the passive tracers case. However, in [25] numerical results were presented, indicating that the presence of inertia enhances further the diffusivity. Thus, we expect that if the effective diffusivity goes to zero in the $\sigma \to 0$ limit, this would happen no faster than linearly, since this is the case for the passive tracers.

We start our investigation as we did in the case of passive tracers by comparing the two methods pathwise. We choose the value of $\sigma = 10^{-2}$ and integrate for $T = 10^4$ with time step $\Delta t = 10^{-2}$, using the same noise realization in the y equations, to obtain Fig. 10.

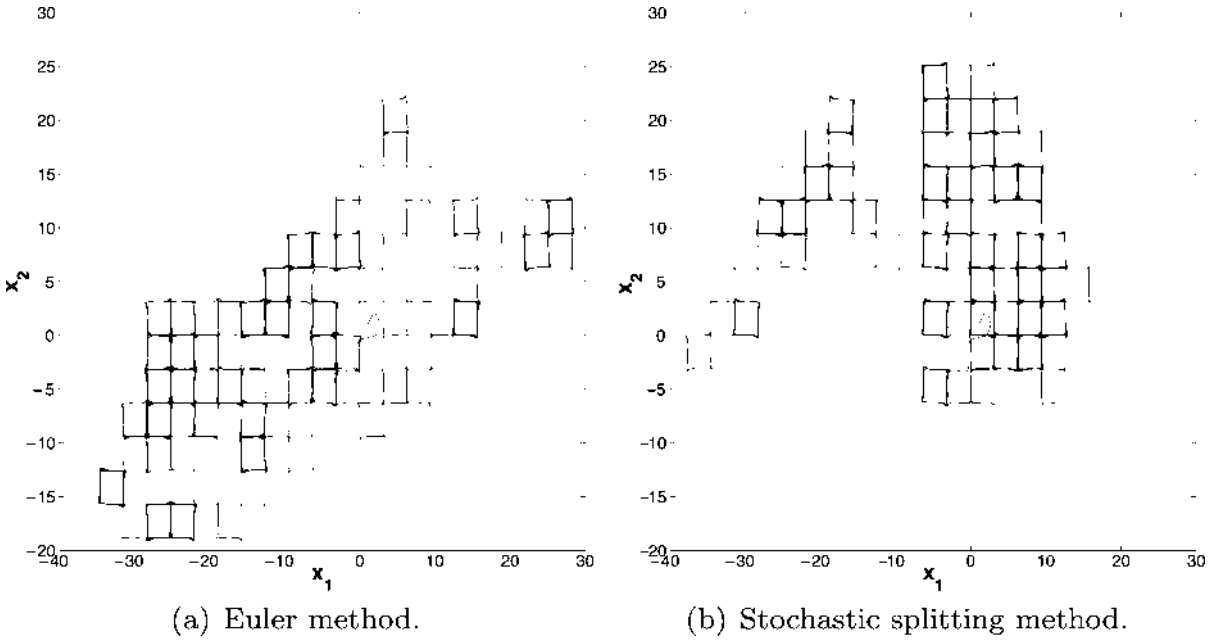

Fig. 10. Phase plane for the two different methods.

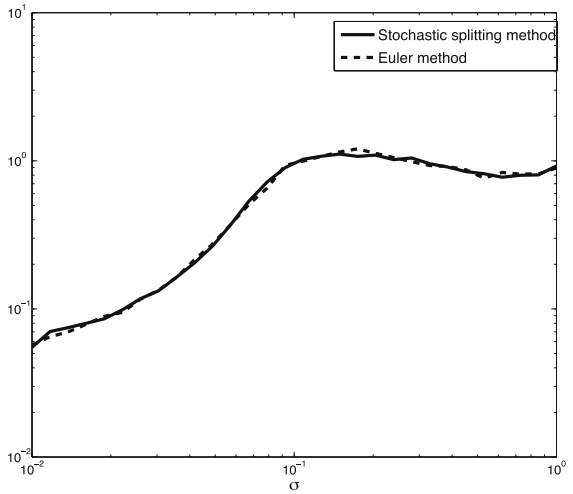

Fig. 11. Effective diffusivity as a function of σ for the two different methods for the Taylor–Green flow, $\tau = 1$.

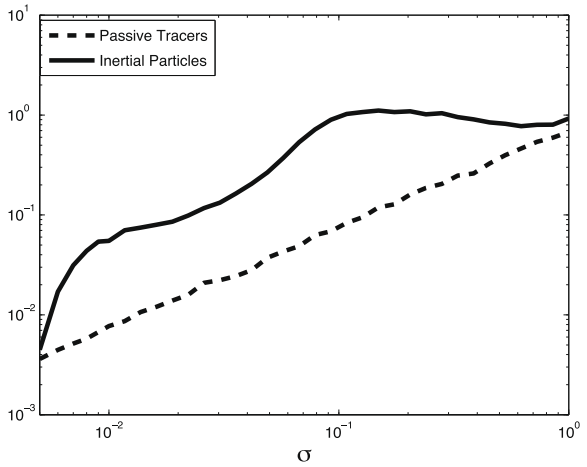

Fig. 12. Comparison of the effective diffusivity: passive tracers vs inertial particles.

As we see in Fig. 10 the qualitative behaviour of the solutions is the same, unlike the passive tracers case. We see in Fig. 11 that the effective diffusivity is the same for the two methods with $\tau = 1$, for values of $\sigma \in [10^{-2}, 1]$. The effective diffusivity has been calculated with time step $\Delta t = 10^{-2}$, final integration time $T = 10^5$, and for $N = 10^3$ realizations.

In Fig. 12 we compare the effective diffusivity of passive tracers and inertial particles in the small diffusion regime, calculated in both cases with the stochastic splitting method. The results are consistent with the conjecture in [25], that the effective diffusivity of inertial particles is always greater than that for passive tracers. Note also that the behaviour of the effective diffusivity as a function of σ in the case of inertial particles is highly nonlinear, unlike the passive tracers case.

Concluding this investigation we see that for the case of inertial particles under the Taylor–Green velocity field, it seems that there is no advantage in using the stochastic splitting method over the Euler–Maryama method in the small molecular diffusivity regime, for τ of $\mathcal{O}(1)$.

6. Numerical investigations: the small inertia case

In this section we study the effect of small inertia on the problem (1.4). We know from Result 10 that the first-order correction to the effective diffusivity matrix is $\mathcal{O}(\sqrt{\tau})$ and that is what we would like our numerical method to reproduce.

As we have previously mentioned, in this regime the Euler method fails to give an accurate calculation of the effective diffusivity, in any reasonable computing time. The reason for this is that we require $\Delta t = \mathcal{O}(\tau)$ in order to avoid numerical instability. This makes the use of the Euler method impractical for very small values of τ. Thus from now on, we only use the stochastic splitting method to investigate the small inertia limit.

Our objectives in this section are:

(i) Illustrate Theorem 2 by means of numerical experiments.
(ii) Study the asymptotic behaviour of the splitting method, for $\tau \ll 1$.
(iii) Study the behaviour of the effective diffusivities for $\tau \ll 1$.

6.1. Shear flow

In this subsection we study the effective diffusivity of inertial particles under the shear flow in the small inertia regime. As we have already seen in Section 4.2 the stochastic splitting method for fixed Δt maintains the pathwise convergence to passive tracers as $\tau \to 0$. This property of the method is illustrated in Fig. 13, where we plot $\sup_{1\le n\Delta t\le T}\|x_n - x_n^\tau\|$ as a function of τ, where $\Delta t = 10^{-3}$, $T = 1$ and $\sigma = 1$. In this case x_n, x_n^τ is the numerical approximation for passive tracers and inertial particles moving in the shear flow, respectively, both calculated using the stochastic splitting method. In order for this comparison to be meaningful we have used the same noise realization in the x equations for the passive tracers and the inertial particles (see the proof of Lemma 13 in the Appendix B), If we now try to fit the data for $\tau \in [10^{-6}, 10^{-4}]$ in Fig. 13, we find that the error reduces like τ^β where $\beta = 0.4955$, which is what we expected from Theorem 2.

We now proceed to investigate what happens for the effective diffusivity of the inertial particles in the small inertia regime for the shear flow. In Fig. 14 we plot the effective diffusivity of the inertial particles for different values of τ and $\sigma = 1$.

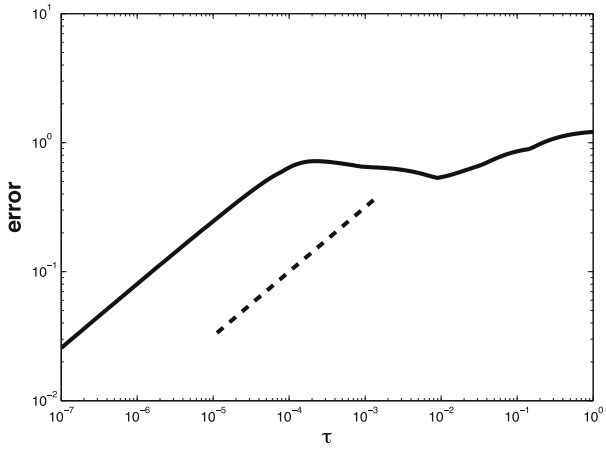

Fig. 13. Log–log plot of the error as a function of τ.

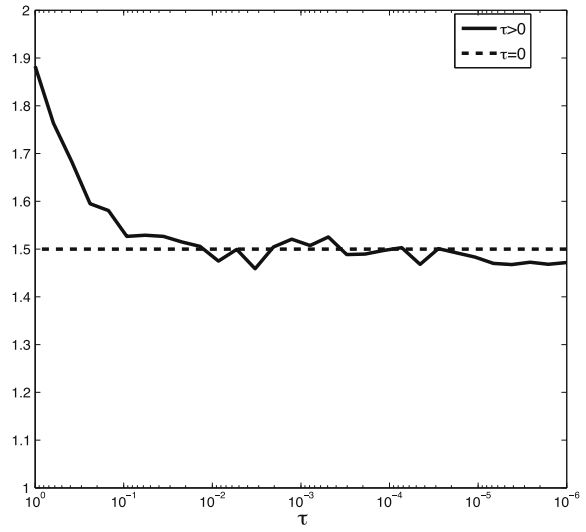

Fig. 14. Effective diffusivity as a function of τ for $\sigma = 1$.

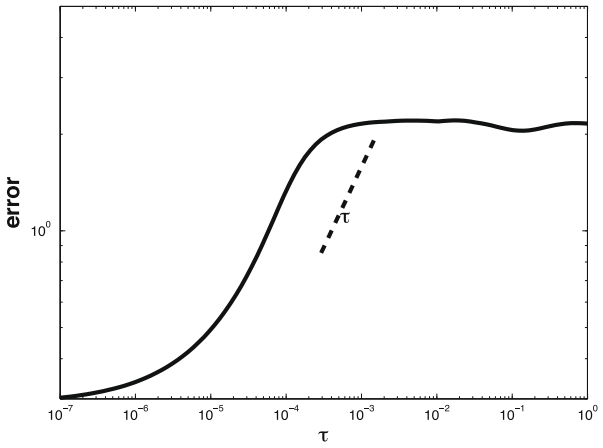

Fig. 15. Log–log plot of the error as a function of τ.

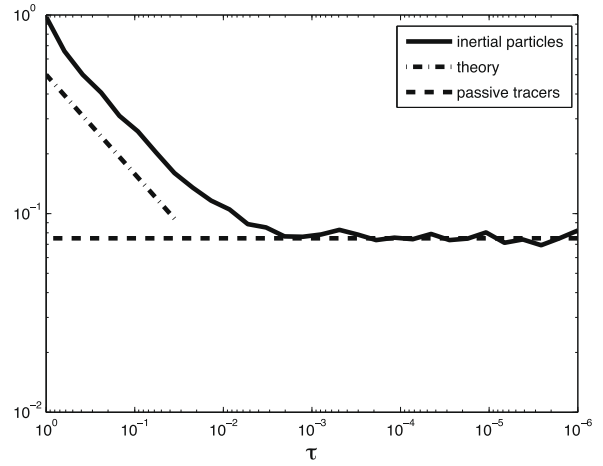

Fig. 16. Effective diffusivity as a function of τ and Δt for $\sigma = 0.1$.

For the calculation of the effective diffusivity we have used $N = 10^4$ realizations with final integration time $T = 10^3$ and time step $\Delta t = 10^{-2}$. The results are consistent with Result 10.

6.2. Taylor–Green velocity field

In this subsection we study the effective diffusivity of inertial particles under the Taylor–Green velocity field in the small inertia regime. In Fig. 15 we plot $\sup_{1\le n\Delta t\le T}\|x_n - x_n^\tau\|$ as a function of τ. Again we have used the same noise in both the passive tracers and the inertial particles equation, as in the case of the shear flow. We have used time step $\Delta t = 10^{-3}$, final integration time $T = 1$ and $\sigma = 1$. If we now fit the data of the figure for values of $\tau \in [10^{-5}, 10^{-3}]$ we find that the error reduces like τ^β, where $\beta = 0.5266$. which is close to the prediction from Theorem 2.

We now proceed with investigating the effective diffusivity in the small τ regime for the Taylor–Green velocity field. In Fig. 16 we plot the effective diffusivity for different values of τ for $\sigma = 0.1$. We have used a final integration time $T = 10^4$ and $N = 10^3$ iterations and time-step $\Delta t = 10^{-3}$. As we can see the effective diffusivity behaves in the expected way (Result 10), since as $\tau \to 0$ it converges to that of passive tracers. Also, if we fit the data for values of $\tau \in [10^{-2}, 5\times 10^{-1}]$, we find that the effective diffusivity reduces like τ^α, where $\alpha = 0.504$, which again is in agreement with Result 10.

7. Numerical investigations: vanishing molecular diffusion and small inertia

In this section we study the limit of both τ and σ going to zero with the special scaling $\sigma = \sqrt{\tau}$ (see Result 11). In this case we have shown using formal asymptotic arguments that the inertial particles for in this particular scaling can be approximated by Eq. (4.10):

$$\dot{x} = v(x) - \tau(\nabla v(x))v(x) + \sqrt{\tau}\dot{\beta}_1.$$

We will refer to this model as the *modified passive tracers model*. The objectives of our investigations in this section are:

(i) Extend the stochastic splitting method to study the effective diffusivity for the modified passive tracers model.
(ii) Deduce properties of the effective diffusivity in this regime.
(iii) Compare the effective diffusivity of the modified passive tracers model with the effective diffusivity of the original passive tracers and of inertial particles and verify the validity of the modified passive tracers model.

7.1. Shear flow

In the limit of vanishing molecular diffusion and small inertia the modified passive tracers model is trivial since

$$(\nabla v(x))v(x) = 0,$$

for the shear flow and so there is no first-order invariant manifold correction. Thus the modified passive tracers model reduces to

$$\dot{x} = v(x) + \sqrt{\tau}\dot{W}.$$

This is precisely the passive tracers models when $\sigma = \sqrt{\tau}$ and the behaviour of the effective diffusivity is analytically known.

7.2. Taylor–Green velocity field

In this subsection we study the Taylor–Green velocity field in the limit of vanishing molecular diffusion and small inertia. The limit in this case is no longer trivial, since

$$(\nabla v(x))v(x) = \frac{1}{2}\begin{pmatrix}\sin 2x_1\\ \sin 2x_2\end{pmatrix}.$$

We study the effective diffusivity for this problem numerically. Since we expect the Euler method to perform poorly on the modified passive tracers equations, we use a generalization of the stochastic splitting method. We perform the first two splitting steps as we did in the case of passive tracers. We then add a third deterministic step, where we add the correction $-\tau(\nabla v(x))v(x)$ and finally add the noise.

Before we proceed with our numerical investigations, we try to get some insight into the effect of the correction term on the individual trajectories. One way of doing this is to study the time derivative of the stream function $\Psi(x_1, x_2) = \sin x_1 \sin x_2$ for Eq. (4.10). Using Itô's formula we obtain

$$\dot{\Psi} = -\tau\Psi(\cos x_1^2 + \cos x_2^2) - \tau\Psi + M, \tag{7.1}$$

where the integral of M is a mean zero martingale. Note that if we compare this equation with (5.6) for $\sigma = \sqrt{\tau}$ we see that we have an extra term in the drift, which as we have already seen in the analysis of the Euler method, is responsible for a spiraling out effect within cells. We thus expect the effective diffusivity of the approximate model to be greater than the effective diffusivity of the passive tracers for the same value of the molecular diffusion coefficient σ.

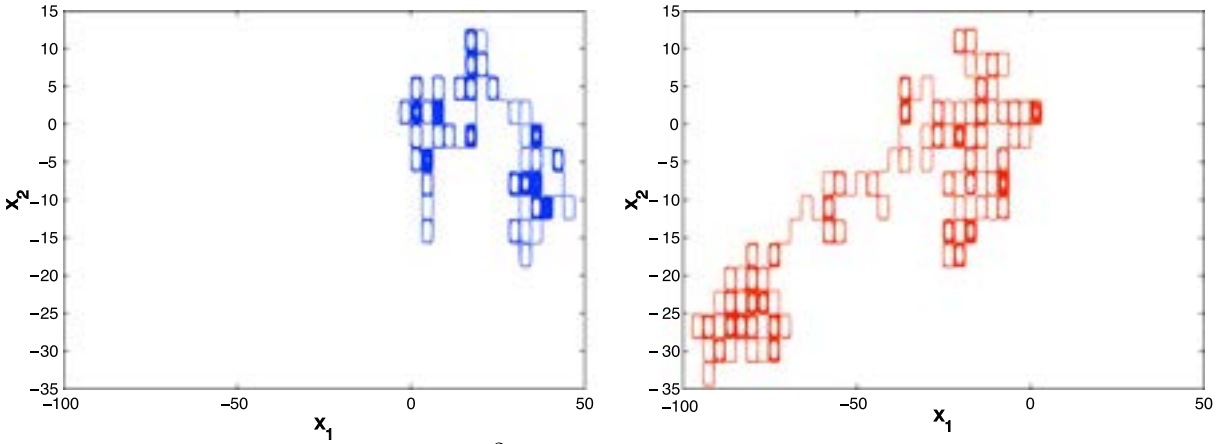

(a) Original passive tracers for $\sigma^2 = \tau$. (b) Modified passive tracers model.

Fig. 17. Phase plane for the modified and the original passive tracers model, $T = 10^4$.

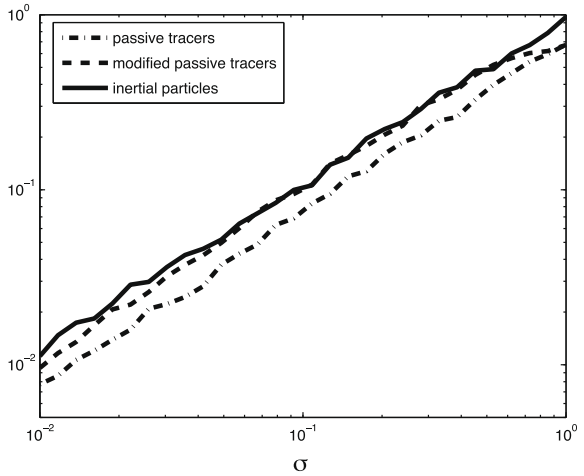

Fig. 18. Effective diffusivity as a function of $\sigma = \sqrt{\tau}$ for the two different passive tracers models.

In Fig. 17 we plot the phase plane for the two different models for final integration time $T = 10^4$ with time step $\Delta t = 10^{-2}$ and for value of $\tau = 10^{-3}$, using the same noise to drive both equations. It is clear that in the case of the approximate model, the particle behaves more diffusively than in the passive tracers model. In Fig. 18 we plot the effective diffusivity as a function of $\sigma = \sqrt{\tau}$ for the approximate model (4.10) as well as for the original inertial particles and passive tracers.

As we see in Fig. 18 the effective diffusivity of the approximate model is larger than the effective diffusivity of the original passive tracers model, as expected. Moreover, the effective diffusivity of the inertial particles in the limit $\tau \to 0$, with $\sigma = \sqrt{\tau}$ is greater, than the effective diffusivity for both modified and original passive tracers. However, the effective diffusivity of the modified passive tracers model captures the full model in the case $\sigma^2 = \tau,\ \tau \to 0$, which verifies the validity of the approximate model, derived in Result 11.

8. Conclusions

The problem of numerically calculating effective diffusivities in the vanishing molecular diffusion limit is studied in this paper. Both passive tracers and inertial particles models are considered. A stochastic splitting method is proposed that takes explicitly into account the features of the equations for passive tracers in the absence of molecular diffusion, building on ideas in [28]. Using this method to calculate the effective diffusivity we find excellent agreement with the existing theoretical predictions. A series of numerical calculations are performed for passive tracers to compare the stochastic splitting method and the Euler method; these numerical tests exhibit the superior behaviour of the stochastic splitting method. These observations are quantified with means of backward error analysis, which reveals the failure of the Euler method to capture the essential dynamics for small molecular diffusion. In the case of inertial particles for Stokes number τ of $\mathcal{O}(1)$, we find no significant advantage of the stochastic splitting method over the Euler method. However, in the limit of small τ we are able to prove that for a fixed timestep Δt the stochastic splitting method maintains the property of pathwise convergence of the inertial particles model to the passive tracers one as $\tau \to 0$, for a fixed final time T. This behaviour is manifested in the numerical calculation of the effective diffusivities, where the correct limiting behaviour is also captured. The combined limit of small inertia and vanishing molecular diffusion is also studied in this paper. A modified passive tracers model that approximates the dynamics of inertial particles in this regime is found by means of formal asymptotics. An extension of the splitting method is used to calculate the effective diffusivity and the results obtained agree with the theoretical predictions.

Acknowledgments

The authors thank the Center for Scientific Computing at Warwick University for computational resources. K.C.Z was supported by Warwick University through the Warwick Postgraduate Research Fellowship (WPRF) and by the EPSRC.

Appendix A

In this appendix we derive the modified passive tracers equation from Result 11. We write (4.9) as the first-order system

$$\dot{x} = y, \tag{A.1a}$$

$$\dot{y} = \frac{1}{\tau} v(x) - \frac{1}{\tau} y + \frac{1}{\sqrt{\tau}} \dot{W}. \tag{A.1b}$$

The generator $\mathcal{L}$ of the Markov process $\{x(t), y(t)\}$ is of the form

$$\mathcal{L} = \frac{1}{\tau}\mathcal{L}_0 + \mathcal{L}_1,$$

where

$$\mathcal{L}_0 = (v(x) - y)\cdot\nabla_y + \frac{1}{2}\Delta_y,$$
$$\mathcal{L}_1 = y\cdot\nabla_x.$$

Note that $\mathcal{L}_0$ is the generator of an Orstein–Uhlenbeck process in y with mean value $v(x)$. The invariant measure of the process is a Gaussian $\mathcal{N}(v(x), \frac{1}{2}I_d)$ where I_d is the d-dimensional unit matrix. From now we use $\langle\cdot\rangle_\rho$ to denote averages with respect to this invariant measure where ρ is the density of this Gaussian measure, which solves the stationary Fokker–Planck equation $\mathcal{L}_0^*\rho = 0$. Note that the Fredholm alternative applies: the null space of the generator $\mathcal{L}_0$ is one-dimensional and consists of constants in x. Moreover, the equation $\mathcal{L}_0 f = g$ has a unique (up to constants) solution if and only if

$$\langle g\rangle_\rho := \int_{\mathbb{R}^d} g(y)\rho(y)dy = 0.$$

Let $X_t^{x,y} := \{x(t), y(t); x(0) = x, y(0) = y\}$ denote the solution of (A.1b) starting at $\{x, y\}$ and let $f : \mathbb{R}^d \times \mathbb{R}^d \mapsto \mathbb{R}$ be a smooth bounded function. Then the function $u^\tau(x, y, t) = \mathbb{E}f(X_t^{x,y})$ satisfies the backward Kolmogorov equation associated with the SDE (A.1b) [22, Chapter 6]

$$\frac{\partial u^\tau}{\partial t} = \left(\frac{1}{\tau}\mathcal{L}_0 + \mathcal{L}_1\right)u^\tau, \quad \text{with } u^\tau|_{t=0} = f. \tag{A.2}$$

We look for a solution of (A.2) in the form of a power series in τ:

$$u^\tau(x, y, t) = u_0(x, y, t) + \tau u_1(x, y, t) + \tau^2 u_2(x, y, t) + \cdots \tag{A.3}$$

We substitute (A.3) in (A.2) and by equating equal powers in τ we obtain the following sequence of equations:

$$-\mathcal{L}_0 u_0 = 0, \tag{A.4a}$$
$$-\mathcal{L}_0 u_1 = \mathcal{L}_1 u_0 - \frac{\partial u_0}{\partial t}, \tag{A.4b}$$
$$-\mathcal{L}_0 u_2 = \mathcal{L}_1 u_1 - \frac{\partial u_1}{\partial t}. \tag{A.4c}$$

From (A.4a), since the process generated by $\mathcal{L}_0$ is ergodic we deduce that the first term in the expansion is independent of y, so $u_0(x, y, t) = u_0(x, t)$. In order for Eq. (A.4b) to have a solution we need

$$\left\langle \mathcal{L}_1 u_0 - \frac{\partial u_0}{\partial t}\right\rangle_\rho = 0$$

and, since u_0 is independent of y

$$\frac{\partial u_0}{\partial t} = \langle y\cdot\nabla_x u_0\rangle_\rho,$$

so that

$$\frac{\partial u_0}{\partial t} = v(x)\cdot\nabla_x u_0.$$

This implies that, to leading order, the dynamics are deterministic, since this is the Liouville equation corresponding to the ODE $\dot{x} = v(x)$, as expected. We now calculate the first-order correction in the expansion (A.3). Eq. (A.4b) becomes

$$-\mathcal{L}_0 u_1 = y\cdot\nabla_x u_0 - v(x)\cdot\nabla_x u_0. \tag{A.5}$$

We can solve this by setting

$$u_1 = \chi(x, y)\cdot\nabla_x u_0 + \Psi(x, t),$$

where the Ψ term belongs to the null space of $\mathcal{L}_0$. We impose the normalization

$$\langle\chi(x, y)\rangle_\rho = 0. \tag{A.6}$$

If we now substitute the expression for u_1 in (A.5) we obtain the cell problem

$$-\mathcal{L}_0\chi = y - v(x), \tag{A.7}$$

which under the condition (A.6) gives the solution $\chi = y - v(x)$ and so

$$u_1 = (y - v(x)) \cdot \nabla_x u_0 + \Psi(x,t).$$

If we now substitute this expression for u_1 into (A.4c) we obtain

$$-\mathcal{L}_0 u_2 = y(y - v(x))^T : \nabla_x \nabla_x u_0 - (\nabla_x v(x) y) \cdot \nabla_x u_0 + y \cdot \nabla_x \Psi - \frac{\partial u_1}{\partial t},$$

and by applying the solvability condition we end up with

$$\left\langle \frac{\partial u_1}{\partial t} \right\rangle_\rho = \langle y(y - v(x))^T : \nabla_x \nabla_x u_0 - (\nabla_x v(x) y) \cdot \nabla_x u_0 + y \cdot \nabla_x \Psi \rangle_\rho.$$

Thus

$$\begin{aligned} \frac{\partial \Psi}{\partial t} &= \langle (y - v(x))(y - v(x))^T : \nabla_x \nabla_x u_0 - (\nabla_x v(x) y) \cdot \nabla_x u_0 + y \cdot \nabla_x \Psi \rangle_\rho + \langle v(x)(y - v(x))^T : \nabla_x \nabla_x u_0 \rangle_\rho, \\ &= -\nabla_x v(x) v(x) \cdot \nabla_x u_0 + v(x) \cdot \nabla_x \Psi + \frac{1}{2} \Delta_x u_0. \end{aligned}$$

If we now set $\widehat{u} = \langle u_0 + \tau u_1 \rangle$, we find that $\widehat{u} = u_0 + \tau \Psi$ and that $\widehat{u}$ satisfies

$$\frac{\partial \widehat{u}}{\partial t} = v(x) \cdot \nabla_x \widehat{u} - \tau (\nabla_x v(x)) v(x) \cdot \nabla_x \widehat{u} + \frac{\tau}{2} \Delta_x \widehat{u} + \mathcal{O}(\tau^2). \tag{A.8}$$

This implies that the effective equation describing the corrections to the Langrangian dynamics is

$$\dot{x} = v(x) - \tau (\nabla_x v(x)) v(x) + \sqrt{\tau} \dot{W},$$

since (A.8) is the backward Kolmogorov equation for this SDE. We reiterate that the derivation of Eq. (A.8) is just formal and is not a proof that solutions to (4.10) are indeed close to solutions to (A.1b). To prove such a result would require more sophisticated techniques, such as those in Part III of [22].

Appendix B

In this appendix we present the two lemmas needed for the proof of Theorem 2.

Lemma 12. *Let $\widehat{\phi}(\widehat{x}, \widehat{y}, \Delta t), \phi(x, \Delta t)$ defined in Eqs. (2.11) and (2.20). Then there exist constants $M,\ K,\ C_1$ independent of $\tau, \Delta t$, such that*

$$P_y \widehat{\phi}(\widehat{x}, \widehat{y}, \Delta t) \le M \quad \text{and} \quad \|P_x \widehat{\phi}(\widehat{x}, \widehat{y}, \Delta t) - \phi(x, \Delta t)\| \le (1 + K\Delta t)\|\widehat{x} - x\| + C_1 \sqrt{\tau}.$$

Proof 4. We start by analyzing the deterministic subequations (2.12), in particular the equation for y. More specifically, we show that $P_y \widehat{\phi}_j(\widehat{x}, \widehat{y}, \Delta) = \mathcal{O}(1)$, uniformly in τ. We have

$$P_y \widehat{\phi}_j(\widehat{x}, \widehat{y}, \Delta t) = \widehat{y} \exp\left(-\frac{t}{(n+1)\tau}\right) + \frac{1}{\sqrt{\tau}} \int_0^{\Delta t} \exp\left(-\frac{\Delta t - s}{(n+1)\tau}\right) f_j(s) ds, \tag{B.1}$$

where

$$f_j(t) = d_j v_j\left(\alpha - b(n+1)\tau \exp\left[-\frac{t}{(n+1)\tau}\right]\right).$$

If we make the substitution $q = e^{\frac{s}{(n+1)\tau}}$ then Eq. (B.1) becomes

$$P_y \widehat{\phi}_j(\widehat{x}, \widehat{y}, \Delta t) = \widehat{y} e^{-\frac{\Delta t}{(n+1)\tau}} + (n+1)\sqrt{\tau} e^{-\frac{\Delta t}{(n+1)\tau}} \int_1^{e^{\frac{\Delta t}{(n+1)\tau}}} d_j v_j\left(a - \frac{b(n+1)\tau}{q}\right) dq,$$

and now since v_j is bounded we deduce that

$$P_y \widehat{\phi}_j(\widehat{x}, \widehat{y}, \Delta t) \le \widehat{y} e^{-\frac{\Delta t}{(n+1)\tau}} + C(n+1)\sqrt{\tau}\left(1 - e^{\frac{-\Delta t}{(n+1)\tau}}\right) \le C_1 \sqrt{\tau}.$$

We now study the x-equation which can be written, using (2.20), as

$$P_x \widehat{\phi}_j(\widehat{x}, \widehat{y}, \Delta t) = \widehat{x} + \sqrt{\tau}\widehat{y}\left(1 - e^{\frac{-\Delta t}{(n+1)\tau}}\right) + \int_0^{\Delta t} \left[1 - e^{-\frac{\Delta t - s}{(n+1)\tau}}\right] f_j(s) ds.$$

The integral on the right-hand side of the above equation can be written as

$$\int_0^{\Delta t} \left[1 - \exp\left(-\frac{\Delta t - s}{(n+1)\tau}\right)\right] f_j(s) ds = \int_0^{\Delta t} f_j(s) ds - \int_0^{\Delta t} \exp\left(-\frac{\Delta t - s}{(n+1)\tau}\right) f_j(s) ds.$$

Now notice that the second part of the integral is the same that appeared in the y-equation multiplied by $\sqrt{\tau}$. Thus we obtain the bound

$$\left|\int_0^{\Delta t} e^{-\frac{\Delta t-s}{(n+1)\tau}} f_j(s)ds\right| \leq C_1\tau. \tag{B.2}$$

Now we have that

$$\int_0^{\Delta t} f_j\big(\langle e_j,\widehat{x}\rangle + (n+1)\tau\langle e_j,\widehat{y}\rangle\big(1-e^{-\frac{s}{\tau}}\big)\big)ds = \Delta t f_j(\langle e_j,\widehat{x}\rangle) + f'(\langle e_j,\widehat{x}\rangle)\int_0^{\Delta t} C_1(n+1)\tau\langle e_j,\widehat{y}\rangle\big(1-e^{-\frac{s}{\tau}}\big)ds, \tag{B.3}$$

where we have taken a Taylor expansion around $\langle e_j, x_j^\tau(0)\rangle$. Thus we have

$$P_x\widehat{\phi}_j(\widehat{x},\widehat{y},\Delta t) = \phi_j(\widehat{x},\Delta t) + \tau\widehat{y}\Big(1-e^{\frac{\Delta t}{(n+1)\tau}}\Big) + f'(\langle e_j,\widehat{x}\rangle)\int_0^{\Delta t} C_1(n+1)\tau\langle e_j,\widehat{y}\rangle\big(1-e^{-\frac{s}{\tau}}\big)ds.$$

Using now the fact that v_j is Lipschitz continuous with constant $L_j \leq L$ for all j and also bounded is easy to see that

$$\|P_x\widehat{\phi}_j(\widehat{x},\widehat{y},\Delta t) - \phi_j(x,\Delta t)\| \leq (1+L_j\Delta t)\|\widehat{x}-x\| + C_1\sqrt{\tau} + C_2\tau\Delta t + C_3\tau^2\Delta t. \tag{B.4}$$

The proof of the first statement of the lemma now follows from (B.2), the bound $|P_y\widehat{\phi}_j(\widehat{x},\widehat{y},\Delta t)| \leq C$, together with the fact that and $P_y\widehat{\phi}(\widehat{x},\widehat{y},\Delta t)$ is given as a composition of every $P_y\widehat{\phi}_j(\widehat{x},\widehat{y},\Delta t)$. In order to prove the second statement we need to use (B.4)

$$\begin{aligned}\|P_x\widehat{\phi}(\widehat{x},\widehat{y},\Delta t) - \phi(x,\Delta t)\| &= \|P_x\widehat{\phi}_n\circ\cdots\widehat{\phi}_1(\widehat{x},\widehat{y},\Delta t) - \phi_n\circ\cdots\phi_1(x,\Delta t)\| \leq (1+L\Delta t)^n\|\widehat{x}-x\| + C_1\sqrt{\tau},\\ &\leq (1+K\Delta t)\|\widehat{x}-x\| + C_1\sqrt{\tau}. \qquad \square\end{aligned}$$

We now study the effect of the additive noise. We have the following lemma:

Lemma 13. *Let $\gamma, g(\gamma,\xi,t)$ denote the random variables that we add in Eqs. (2.11) and (2.20). Then there exist a constant M independent of $\Delta t, \tau$*

$$\mathbb{E}(\|P_x g(\gamma,\xi,t) - \sigma W(t)\|)^2 \leq M\tau. \tag{B.5}$$

Proof 5. We can solve (2.16b) to obtain

$$\begin{aligned}x^\tau(t) &= x^\tau(0) + \sqrt{\tau}\Big(1-e^{\frac{-t}{(n+1)\tau}}\Big)y(0) + \sigma\int_0^t\Big(1-e^{-\frac{t-s}{(n+1)\tau}}\Big)dW_s,\\ y(t) &= y(0)e^{\frac{-t}{(n+1)\tau}} + \frac{\sigma}{\sqrt{\tau}}\int_0^t e^{-\frac{t-s}{(n+1)\tau}}dW_s.\end{aligned}$$

Thus

$$P_x g(\gamma,\xi,t) = \sigma\int_0^t\Big(1-e^{-\frac{t-s}{(n+1)\tau}}\Big)dW_s,$$

where

$$\gamma = \frac{1}{\sqrt{t}}W_t.$$

Thus, and upon noticing that $\sqrt{(}t)\gamma = W(t)$,

$$\mathbb{E}(\|P_x g(\gamma,\xi,t) - \sigma W(t)\|)^2 = \sigma^2\int_0^t e^{-\frac{2(t-s)}{(n+1)\tau}}ds = \frac{\sigma^2(n+1)\tau}{2}\Big(1-e^{-\frac{2t}{(n+1)\tau}}\Big) \leq M\tau,$$

and the proof is complete. $\square$

Appendix C

In this appendix we prove the lemma needed for the proof of Theorem 1.

Lemma 14. *Let $\widehat{y}_n$ denote the numerical approximation of (3.1) at time $n\Delta t$ using the Euler–Maryama method and y_n approximation for the splitting method at $n\Delta t$ and the same realization of the noise. Then there exists a positive constant $C(T)$ depending only on T such that*

$$\left(\mathbb{E}\sup_{0\le n\Delta t\le T}|\widehat{y}_n - y_n|^2\right)^{1/2} \le C(T)\Delta t. \tag{C.1}$$

Proof 6. We prove this lemma in the case where the velocity field can be split into two parts

$$F(z) = F_1(z) + F_2(z).$$

The generalization to the case where the velocity field is splitted into more than two parts is straightforward. We remark that Condition (2.4) is not needed for the proof of this lemma. The Euler approximation gives

$$\widehat{y}_{n+1} = \widehat{y}_n + \Delta t F(\widehat{y}_n) + \Sigma\sqrt{\Delta t}\gamma_n, \tag{C.2}$$

where $\gamma_n \sim \mathcal{N}(0, I_d)$. The splitting method on the other hand has three steps:

$$\begin{aligned} y_n^1 &= y_n + \Delta t F_1(y_n),\\ y_n^2 &= y_n^1 + \Delta t F_2(y_n^1),\\ y_{n+1} &= y_n^2 + \Sigma\sqrt{\Delta t}\gamma_n. \end{aligned}$$

Here γ_n is the same random variable as in the Euler approximation, since we compare solutions with the same realization of the noise. If we now compose these three steps we obtain

$$y_{n+1} = y_n + \Delta t F_1(y_n) + \Delta t F_2(y_n + \Delta t F_1(y_n)) + \Sigma\sqrt{\Delta t}\gamma_n.$$

If we do a first-order Taylor expansion we obtain

$$y_{n+1} = y_n + \Delta t F_1(y_n) + \Delta t F_2(y_n) + \Sigma\sqrt{\Delta t}\gamma_n + C_n\Delta t^2 = y_n + \Delta t F(y_n) + \Sigma\sqrt{\Delta t}\gamma_n + C_n\Delta t^2. \tag{C.3}$$

Here $\sup_n|C_n| \le C$ where C is independent of Δt, T and of the random driving white noise. We now define with $e_n = y_n - \widehat{y}_n$ and subtract Eq. (C.2) from (C.3) to obtain

$$e_{n+1} = e_n + \Delta t(F(y_n) - F(\widehat{y}_n)) + C_n\Delta t^2,$$

and now by taking the inner product of e_{n+1} with itself

$$\begin{aligned} |e_{n+1}|^2 &\le \langle e_n, e_{n+1}\rangle + \Delta t\langle F(y_n) - F(\widehat{y}_n), e_{n+1}\rangle + \langle C_n\Delta t^2, e_{n+1}\rangle,\\ &\le \frac{1}{2}|e_n|^2 + \frac{1}{2}|e_{n+1}|^2 + \Delta t|F(y_n) - F(\widehat{y}_n)||e_{n+1}| + \langle C_n\Delta t^{3/2}, \Delta t^{1/2}e_{n+1}\rangle,\\ &\le \frac{1}{2}|e_n|^2 + \frac{1}{2}|e_{n+1}|^2 + \Delta t L|e_n||e_{n+1}| + \frac{\Delta t^3}{2}|C_n|^2 + \frac{\Delta t}{2}|e_{n+1}|^2,\\ &\le \frac{1}{2}|e_n|^2 + \frac{1}{2}|e_{n+1}|^2 + \frac{L\Delta t}{2}|e_n|^2 + \frac{L\Delta t}{2}|e_{n+1}|^2 + \frac{C^2\Delta t^3}{2} + \frac{\Delta t}{2}|e_{n+1}|^2. \end{aligned}$$

Now by taking $|e_{n+1}|^2$ to the left-hand side we obtain

$$(1 - (L+1)\Delta t)|e_{n+1}|^2 \le (1 + L\Delta t)|e_n|^2 + C^2\Delta t^3.$$

Setting $e_0 = y_0 - \widehat{y}_0 = 0$ we obtain by induction

$$|e_n|^2 \le C^2\Delta t^3\sum_{k=0}^{n-1}\left(\frac{1 + L\Delta t}{1 - (1+L)\Delta t}\right)^k, \le C^2\Delta t^3\sum_{k=0}^{n-1}(1 + L\Delta t)^k, \le C^2\Delta t^3\frac{(1 + L\Delta t)^n - 1}{1 + L\Delta t - 1},$$

and by taking supremum over n and then expectations we finally obtain

$$\mathbb{E}\left(\sup_n|e_n|^2\right) \le \frac{C^2(e^{LT} - 1)}{L}\Delta t^2.$$

Hence we obtained that

$$\left(\mathbb{E}\sup_{0\le n\Delta t\le T}|\widehat{y}_n - y_n|^2\right)^{1/2} \le C(T)\Delta t.$$

Appendix D

In this appendix we calculate the constants α, β, δ used to approximate the stochastic integrals in Section 2.2. These calculations are similar in nature with the ones in [27], while the general framework for calculations of this kind was developed in [26].

We will use the notation

$$I = \frac{\sigma}{\sqrt{\tau}} \int_0^{\Delta t} e^{-\frac{\Delta t - s}{(n+1)\tau}} dW_s, \quad J = \sigma \int_0^{\Delta t} \left(1 - e^{-\frac{\Delta t - s}{(n+1)\tau}}\right) dW_s.$$

It is clear that I, J are correlated Gaussian random variables, since in order to obtain J we need to take the integral of I over time. We can write $I = \beta\xi$ and $J = \alpha\xi + \delta\gamma$ where ξ, γ are independent standard Gaussian random variables. The coefficients α, β, δ can be calculated from the following formulas:

$$\alpha^2 + \delta^2 = \mathbb{E}J^2, \quad \beta\alpha = \mathbb{E}IJ, \quad \beta^2 = \mathbb{E}I^2. \tag{D.1}$$

Calculating now the expectation values in (D.1) we obtain

$$\alpha^2 + \delta^2 = \sigma^2 \left[\Delta t - 2(n+1)\tau(1 - e^{-\frac{\Delta t}{(n+1)\tau}}) + \frac{(n+1)\tau}{2}(1 - e^{-\frac{2\Delta t}{(n+1)\tau}})\right],$$

$$\beta\alpha = \frac{\sigma^2\sqrt{\tau}(n+1)}{2}\left[1 - e^{-\frac{\Delta t}{(n+1)\tau}}\right]^2,$$

$$\beta^2 = \frac{(n+1)\sigma^2}{2}\left[1 - e^{-\frac{2\Delta t}{(n+1)\tau}}\right].$$

References

[1] J. Bec, M. Cencini, R. Hillerbrand, K. Turitsyn, Stochastic suspensions of heavy particles, Phys. D 237 (2008) 2037–2050.
[2] A. Bensoussan, J. Lions, G. Papanicolaou, Asymptotic Analysis of Periodic Structures, North-Holland, Amsterdam, 1978.
[3] R. Carmona, L. Xu, Homogenization theory for time-dependent two-dimensional incompressible Gaussian flows, Ann. Appl. Prob. 7 (1) (1997) 265–279.
[4] P. Castiglione, A. Crisanti, Dispersion of passive tracers in a velocity field with non-δ-correlated noise, Phys. Rev. E 59 (4) (1999) 3926–3934.
[5] G.T. Csanady, Turbulent Diffusion in the Environment, D. Reidel, Dordrecht, 1973.
[6] G. Falkovich, A. Fouxon, M. Stepanov, Acceleration of rain initiation by cloud turbulence, Nature 419 (2002) 151–154.
[7] G. Falkovich, K. Gawędzki, M. Vergassola, Particles and fields in fluid turbulence, Rev. Modern Phys. 73 (4) (2001) 913–975.
[8] A. Fannjiang, Time scales in homogenization of periodic flows with vanishing molecular diffusion, J. Differen. Equat. 179 (2) (2002) 433–455.
[9] A. Fannjiang, G. Papanicolaou, Convection enhanced diffusion for periodic flows, SIAM J. Appl. Math. 54 (1994) 333–408.
[10] E. Hairer, C. Lubich, G. Wanner, Geometric Numerical Integration, Springer Series in Computational Mathematics, vol. 31, Springer-Verlag, Berlin, 2002.
[11] P. Kloeden, E. Platen, Numerical Solution of Stochastic Differential Equations, Applications of Mathematics (New York), vol. 23, Springer-Verlag, Berlin, 1992.
[12] L. Koralov, Random perturbations of 2-dimensional Hamiltonian flows, Probab. Theory Related Fields 129 (1) (2004) 37–62.
[13] A. Majda, P. Kramer, Simplified models for turbulent diffusion: theory, numerical modelling and physical phenomena, Phys. Rep. 314 (1999) 237–574.
[14] M. Maxey, Gravitational settling of aerosol particles in homogeneous turbulence and random flow fields, J. Fluid Mech. 174 (1987) 441–465.
[15] M. Maxey, The motion of small spherical particles in a cellular flow field, Phys. Fluids 30 (7) (1987) 1915–1928.
[16] M. Maxey, On the advection of spherical and nonspherical particles in a nonuniform flow, Philos. Trans. Roy. Soc. London Ser. A 333 (1631) (1990) 289–307.
[17] M. Maxey, J. Riley, Equation of motion for a small rigid sphere in a nonuniform flow, Phys. Fluids 26 (1983) 883–889.
[18] D. McLaughlin, G. Papanicolaou, O. Pironneau, Convection of microstructure and related problems, SIAM J. Appl. Math 45 (1985) 780–797.
[19] H.K. Moffat, Transport effects associated with turbulence with particular attention to the influence of helicity, Rep. Prog. Phys. 46 (1983) 1699–1704.
[20] H. Owhadi, N. Bou-Rabee, Boltzmann–Gibbs preserving Langevin integrators, preprint.
[21] G.A. Pavliotis, A.M. Stuart, K.C. Zygalakis, Homogenization for inertial particles moving in a random flow, Comm. Math. Sci. 5 (3) (2007) 507–531.
[22] G.A. Pavliotis, A.M. Stuart, Multiscale Methods: Averaging and Homogenization, Springer-Verlag, New York, 2008.
[23] G.A. Pavliotis, A.M. Stuart, L. Band, Monte Carlo studies of effective diffusivities for inertial particles, in: Monte Carlo and Quasi-Monte Carlo Methods 2004, Springer, Berlin, 2006, pp. 431–441.
[24] G.A. Pavliotis, A.M. Stuart, White noise limits for inertial particles in a random field, Multiscale Model. Simulat. 1 (4) (2003) 527–533 (electronic).
[25] G.A. Pavliotis, A.M. Stuart, Periodic homogenization for inertial particles, Phys. D 204 (3–4) (2005) 161–187.
[26] Y. Pokern, Fitting Stochastic Differential Equations to Molecular Dynamics Data, PhD Thesis, University of Warwick, Coventry, 2007.
[27] Y. Pokern, A.M. Stuart, P. Wiberg, Parameter estimation for partially observed hypo-elliptic diffusions JRSSB (in press).
[28] G. Quispel, D. McLaren, Explicit volume-preserving and symplectic integrators for trigonometric polynomial flows, J. Comp. Phys 186 (2003) 308–316.
[29] J. Rubin, C.K.R.T. Jones, M. Maxey, Settling and asymptotic motion of aerosol particles in a cellular flow field, J. Nonlinear Sci. 5 (4) (1995) 337–358.
[30] T. Shardlow, Modified equations for stochastic differential equations, BIT 46 (1) (2006) 111–125.
[31] R.A. Shaw, Particle–turbulence interactions in atmosphere clouds, Annu. Rev. Fluid Mech. 35 (2003) 183–227.
[32] B.I. Shraiman, Diffusive transport in a Rayleigh–Benard convection cell, Phys. Rev. A 36 (1) (1987) 261–267.
[33] H. Sigurgeirsson, A.M. Stuart, Inertial particles in a random field, Stoch. Dyn. 2 (2) (2002) 295–310.
[34] H. Sigurgeirsson, A.M. Stuart, A model for preferential concentration, Phys. Fluids 14 (12) (2002) 4352–4361.
[35] A. Soward, Fast dynamo action in a steady flow, J. Fluid Mech. 180 (1987) 267–295.
[36] M. Vergassola, M. Avellaneda, Scalar transport in compressible flow, Physica D 106 (1-2) (1997) 148–166.
[37] L. Wang, M. Maxey, T. Burton, D. Stock, Chaotic dynamics of particle dispersion in fluids, Phys. Fluids A 4 (8) (1992) 1789–1804.
[38] K.C. Zygalakis, Effective Diffusive Behavior For Passive Tracers and Inertial Particles: Homogenization and Numerical Algorithms, PhD Thesis, University of Warwick, Coventry (in preparation).